

Copyright Undertaking

This thesis is protected by copyright, with all rights reserved.

By reading and using the thesis, the reader understands and agrees to the following terms:

1. The reader will abide by the rules and legal ordinances governing copyright regarding the use of the thesis.
2. The reader will use the thesis for the purpose of research or private study only and not for distribution or further reproduction or any other purpose.
3. The reader agrees to indemnify and hold the University harmless from and against any loss, damage, cost, liability or expenses arising from copyright infringement or unauthorized usage.

If you have reasons to believe that any materials in this thesis are deemed not suitable to be distributed in this form, or a copyright owner having difficulty with the material being included in our database, please contact lbsys@polyu.edu.hk providing details. The Library will look into your claim and consider taking remedial action upon receipt of the written requests.

Study of Self-focused Piezoelectric Transducer for Liquid Ejection

Hon Sau Fong

M.Phil

The Hong Kong Polytechnic University

2010

The Hong Kong Polytechnic University
Department of Applied Physics

**Study of Self-focused Piezoelectric Transducer
for Liquid Ejection**

Hon Sau Fong

A thesis submitted in partial fulfilment of the requirements for the degree of

Master of Philosophy

August 2009

Certificate of Originality

I hereby declare that this thesis is my own work and that, to the best of my knowledge and belief, it reproduces no material previously published or written nor material which has been accepted for the award of any other degree or diploma, except where due acknowledgement has been made in the text.

_____ (Signature)

(Name of student)



Abstract

The main objective of the present work is to develop and fabricate focused acoustic ejectors for ejecting drops of viscous liquids in the drop-on-demand mode. To date, most of the ejecting systems for viscous liquids are large and complicated, in particular their electronic driving systems. The newly developed focused acoustic ejectors in the present work are more compact in size and can be operated using simple an electronic driving system. It is anticipated that the ejectors will find various applications in microelectronic packaging.

Fresnel zone plates have been designed and fabricated using lead zirconate titanate piezoelectric plates as the self-focused piezoelectric transducers for the acoustic ejectors. Because of the annular structure of the electrodes, the acoustic waves generated by the piezoelectric plate of the Fresnel zone plate are in phase at the designed focal points. As a result, constructively interfere occurs and the intensity is increased. Our results of the distributions of wave intensity in glycerin (with a viscosity of 1400 cP) clearly reveal two focal points, at which the intensity is higher than the surroundings. The observed focal lengths are about 2.48 and 9.5 mm, which agree with the theoretical values. The observed focal spot is small, having a diameter close to the wavelength of the acoustic wave (0.448 mm). The Fresnel zone plates are operated at 4.28 MHz and the sound



velocity of glycerin is 1920 m/s. Our results also reveal that after the milling of the un-electroded region of the piezoelectric plate, the vibration and hence the wave intensity is enhanced. The number of the annular electrodes does not have significant effects on the wave intensity. However, the acoustic wave is highly attenuated by the viscous liquids, causing the intensity at the principle focal point (9.5 mm) being smaller than that at the “harmonic” focal point (2.48 mm).

On the basis of the results, milled Fresnel zone plates with four annular electrodes are used for the fabrication of the focused acoustic ejectors. The ejectors are driven by a simple electrical signal, a series of tone bursts of sinusoidal wave. The ejection performances of the focused acoustic ejectors using glycerin as the medium have been evaluated in detail. Based on the results, the optimum operation parameters, including the driving voltage and duration of the tone burst, have been determined. Our results reveal that the ejector can eject glycerin in the downward orientation using a tone burst with a frequency of 4.28 MHz, a driving voltage of 35 V and a duration of 2 ms. The drop is small, having a diameter of 0.4 mm which is close to the wavelength of the acoustic wave. Using the same operation parameters, the ejector can eject drops in the drop-on-demand mode. The repetition frequency can be increased to 120 Hz, while the temperature remains at about 50°C.



Besides glycerin, other viscous liquids, such as the pre-polymer of an epoxy (2000 cP) and a detergent, have been used for the evaluation of the ejection performance, and good results are obtained. Similar to glycerin, both the viscous liquids can be ejected effectively in the drop-on-demand mode using a similar tone-burst signal. It is suggested that since only a small volume of the liquid is deformed, the focused acoustic wave is strong enough to stretch the liquid significantly until the surface tension is overcome. As a result, a liquid drop is formed and ejected. Our results also demonstrate that viscosity is more important than the surface tension in controlling the drop ejection.



List of Publications

S. F. Hon and K. W. Kwok, “Study of Piezoelectric Transducer for Liquid Ejection”,
IEEE International Frequency Control Symposium 2009 Joint with the 22nd European
Frequency and Time forum 2009, pp. 1050 - 1054



Acknowledgements

I would like to express my sincere gratitude to my supervisor, Dr. K. W. Kwok for his continuous interest, kindly support and invaluable guidance during this study.

I am also indebted to the colleagues in the ASM International group, particularly to Mr. Peter Ng, Mr. Marcy Lee, Mr. Derek Lai and Mr. Peter Yu for their useful discussions of the design.

I would also like to thank senior artisan Mr. K. H. Ho for the technical support throughout the work.

I gratefully acknowledge from the Research Committee and the Centre for Smart Materials of The Hong Kong Polytechnic University.

Finally, I would like to thank my family for their encouragement.



Table of Content

Abstract	ii
List of Publications	iv
Acknowledgements	v
Table of Content	vi
List of Figure Captions	viii
List of Table Captions	xiii
Nomenclature	xiv
Chapter 1 Introduction	1-1
1.1 Liquid ejections	1-1
1.1.1 Ejection modes	1-1
1.1.2 Ejection of viscous liquids	1-4
1.2 Piezoelectric ejection	1-9
1.2.1 Mechanisms of piezoelectric ejectors	1-9
1.2.2 Advantages of piezoelectric ejectors	1-15
1.2.3 Ejection of various liquids	1-15
1.3 Focused acoustic ejection	1-17
1.3.1 Focused acoustic ejectors	1-17
1.3.2 Focusing elements	1-21
1.3.3 Advantages of Focused acoustic ejection	1-29
1.4 Piezoelectricity	1-31
1.5 Scope of work	1-35
Chapter 2 Design and fabrication of the Fresnel zone plates	2-1
2.1 Design of the Fresnel zone plate	2-3
2.1.1 Theory	2-3
2.1.2 The Fresnel approximation	2-5
2.2 Fabrication of the Fresnel zone plate	2-8
Chapter 3 Characterization of the Fresnel zone plates	3-1
3.1 Measurements of intensity distribution	3-1
3.2 Experimental setup	3-3
3.3 Results and discussion	3-4
3.3.1 Axial intensity distribution	3-4
3.3.2 Transverse intensity distribution	3-8



3.3.3 Comparison of the milled and non-milled FZPs	3-10
Chapter 4 Fabrication and Characterization of Focused Acoustic Ejectors	4-1
4.1 Fabrication of focused acoustic ejectors	4-1
4.2 Characterization of focused acoustic ejectors	4-2
4.3 Results and discussion	4-4
4.3.1 Upward ejection	4-4
4.3.2 Downward ejection	4-7
4.3.3 Effects of the operation parameters	4-10
4.3.3.1 Driving voltage	4-10
4.3.3.2 Tone-burst duration	4-14
4.3.3.3 Repetition frequency	4-17
4.3.3.4 Pressure	4-19
4.3.4 Effects of the ejector design	4-22
4.3.4.1 Orifice size	4-22
4.3.4.2 Operation frequency	4-22
4.3.4.3 Milling of the Fresnel zone plates	4-24
4.3.4.4 Thin copper cover plate	4-25
4.3.4.5 Number of Fresnel zones	4-27
4.3.4.6 Air bubbles	4-29
4.3.5 Ejection of various liquids	4-30
Chapter 5 Conclusion	6-1
Reference	R-1



List of Figure Captions

Fig. 1-1	Drawing of the first liquid ejector in continuous ejection mode [Sweet, 1963]	1-2
Fig. 1-2	Drawing of the electrostatic pull inkjet ejector, which was the first ejector in drop-on-demand mode [Umezu et al., 2005]	1-3
Fig. 1-3	Dispensing distance of contact mode ejection can cause inconsistent drops. (a) too short dispensing distance (b) too long dispensing distance [Lewis et al., 1999]	1-6
Fig. 1-4	Schematic diagrams of (a) Time pressure ejection (b) Auger pump ejection (c) Piston pump ejection [Li et al., 2004]	1-7
Fig. 1-5	Schematic diagram of Jetting dispensing [Li et al., 2004]	1-9
Fig. 1-6	Drawing of the first piezoelectric ejector deforms in squeeze mode. [Zoltan et al., 1970]	1-11
Fig. 1-7	Schematic diagram of the piezoelectric ejector deforms in bend mode	1-12
Fig. 1-8	Schematic diagram of the piezoelectric ejector deforms in push mode	1-12
Fig. 1-9	Schematic diagram of the piezoelectric annular ejector which utilizes the ultrasonic wave to vibrate the copper membrane [Lam et al., 2004]	1-14
Fig. 1-10	Schematic diagram of the piezoelectric ejector utilizing ultrasonic wave to eject the drops [Demirci et al., 2006]	1-14
Fig. 1-11	Drawings of (a) the curved transducer generated several drops simultaneously [Lovelady et al. 1979] and (b) the focused acoustic ejector composed of acoustic lens and transducer [Elrod et al., 1989]	1-17



Fig. 1-12	The commercial focused acoustic ejectors: (a) ATS-100 [Forbush, EDC Biosystem] (b) Portail 630 Reagent multi-spotter [Pickett et al. 2006] (c) acoustic multi ejector printhead [Hadimioglu et al., 2001]	1-20
Fig. 1-13	SEM diagram of Fresnel (phase) acoustic lens fabricated by reactive ion etching [Milster, 2009]	1-21
Fig. 1-14	Schematic diagram of phased delayed system [Kawanami, 2001]	1-23
Fig. 1-15	Photograph of the stainless steel micro-machined FZP for ultrasonic focusing [Schindel, 1997]	1-24
Fig. 1-16	Schematic diagram of the micromachined self-focused acoustic ejector with ZnO FZP [Huang et al., 2001]	1-26
Fig. 1-17	Diagram of the “Incomplete” FZP for directional drop ejection [Kwon et al., 2002]	1-26
Fig. 1-18	Schematic diagram of self-focused acoustic ejector ejecting oil drops from oil-water composite liquid [Yu et al., 2005]	1-27
Fig. 1-19	Schematic diagram of the self-focused acoustic ejector employing air reflector which blocks the propagation of part of acoustic wave for self-focusing [Lee et al., 2006]	1-28
Fig. 1-20	Photograph of the self-focused acoustic ejectors designed for different harmonic frequencies to generate smaller drops [Lee et al., 2008]	1-29
Fig. 1-21	(a) Converse piezoelectric effect and (b) direct piezoelectric effect of piezoelectric material	1-33
Fig. 2-1	(a) Converging and (b) diverging properties with multi-foci of FZP [Milster, 2009]	2-2



Fig. 2-2	The FZP patterned on the piezoelectric plate to self-focus the acoustic waves	2-3
Fig. 2-3	Effect of path difference on wave interference with FZP	2-5
Fig. 2-4	The three diffraction regions: Rayleigh Sommerfeld region, Fresnel region and Fraunhofer region	2-7
Fig. 2-5	Photograph of a milled FZP	2-9
Fig. 3-1	Schematic diagram of the experimental setup to measure the intensity distribution of the acoustic waves in the glycerin	3-4
Fig. 3-2	The variations of intensity (in terms of V_h/V_a) along the axial direction for the milled FZP with six annular electrodes (including the central circular electrode)	3-5
Fig. 3-3	The axial distributions of intensity for the FZPs with six (---■---), five (---*---), four (---△---) annular electrode	3-7
Fig. 3-4	The variations of intensity (in terms of V_h/V_a) along the lateral direction for the milled FZPs with six (---■---), five (---*---), four (---△---) annular electrodes	3-9
Fig. 3-5	The variations of intensity (in terms of V_h/V_a) along the (a) axial direction and (b) transverse direction for the non-milled FZP with four annular electrodes	3-11
Fig. 3-6	Comparisons of the variations of intensity (in terms of V_h/V_a) along the (a) axial direction and (b) transverse direction for the non-milled (---▼---) and milled (---▲---) FZPs with four annular electrodes	3-12
Fig. 4-1	Schematic diagram of the focused acoustic ejector in downward ejection	4-2
Fig. 4-2	Schematic diagram of the experimental setup for evaluating the	4-3



ejection performances of the focused acoustic ejectors

- Fig. 4-3 The wave train comprising of a series of tone bursts with repetition frequency f_{rep} . Each tone burst has voltage V_o , operation frequency f_{op} and duration T 4-3
- Fig. 4-4 Both positions of (a) 2.5 mm and (b) 6 mm can generally observe drop ejection 4-5
- Fig. 4-5 When the liquid depth is not at the focal length (which is higher than L_b), the liquid at the surface is deformed without forming a drop, even though the higher energy of tone burst is used ($V_o = 40$ V and $T = 3$ ms). Photographs (a)-(i) shows the liquid surface deformation with time. Each photograph was taken with time step of $1/600$ s. 4-6
- Fig. 4-6 Downward ejection of glycerin drops in the drop-on-demand mode by the focused acoustic ejector. The operation parameters for the ejection are listed in Table 4-1 4-8
- Fig. 4-7 Photographs showing the deformation of liquid under a driving voltage which is below the threshold value. (a) upward ejection and (b) downward ejection 4-11
- Fig. 4-8 Variation of the velocity of the ejected drops with the driving voltage 4-13
- Fig. 4-9 The maximum height that drop can reach at (a) 30 V (b) 35 V (c) 40 V with $T = 2$ ms 4-13
- Fig. 4-10 Glycerin ejection with driven voltage of (a) 34 V (no drop ejection), (b) 36 V (formation of monodispense drop) and (c) 43 V (drop accompanying with satellite drop) 4-14
- Fig. 4-11 Change of droplet size with tone-burst duration of (a) 1ms (b) 2ms (c) 3ms (d) 4 ms (e) 5ms in downward ejection at the same driving voltage 4-15



Fig. 4-12	The deformed liquid forms a column with height of 10-15 mm with $T = 5$ ms and $V_o = 40$ V	4-16
Fig. 4-13	Downward ejection of different repetition frequency of (a) 50 Hz (b) 80 Hz (c) 100 Hz (d) 120 Hz with the same $V_o = 35$ V and $T = 2$ ms	4-18
Fig. 4-14	Schematic diagram of the desired shape of the meniscus at the orifice needed for the drop ejection	4-20
Fig. 4-15	Meniscus shape of downward ejection of the ejector (a) without metal ring (b) with metal. Photographs (b)-(d) showing the change of shape of meniscus with time during ejection (with time step of $1/600$ s)	4-21
Fig. 4-16	Downward ejections at different operation frequencies of (a) 2.14 MHz (b) 4.28 MHz	4-23
Fig. 4-17	Photographs taken from the ejector with (a) non-milled FZP and (b) milled FZP. Ripples were observed in glycerin surface near the central focal spot for the ejector with non-milled FZP	4-25
Fig. 4-18	(a)-(h) Upward ejection of pre-polymer of epoxy with time (Each photograph was taken with time step of $1/600$ s)	4-33
Fig. 4-19	Downward ejection of pre-polymer in drop on demand mode with $V_o = 40$ V, $T = 2$ ms and $f_{\text{req,max}} = 80$ Hz	4-34
Fig. 4-20	(a)-(h) Upward ejection of detergent with time (Each photograph was taken with time step of $1/300$ s)	4-36



List of Table Captions

Table 1-1	Physical and piezoelectric properties of piezoelectric material APC 880	1-32
Table 1-2	Summary of the ejection conditions and performances of self-focused acoustic ejector	1-37
Table 4-1	Operation parameters for the focused acoustic ejector to eject glycerin drop in the drop-on-demand mode. The focused acoustic ejector is fabricated using the milled FZP with four annular electrodes	4-8
Table 4-2	Normalized droplet diameters for different works	4-10
Table 4-3	Operation condition for ejectors with different number of annular electrodes	4-28
Table 4-4	Operation conditions for ejector ejecting various liquids	4-31



$F_{a, b, c}$	Observed Focal Points
F_d	Designed Focal Point
L	Focal Length
L_d	Designed Focal Length
$L_{a, b, c}$	Observed Focal Length
$L_{1, 2, 3 \dots}$	Calculated Focal Lengths under Fresnel approximation
T	Tone-burst duration
V_a	Voltage applied on Fresnel zone plate
V_h	Measured voltage of a needle-type hydrophone
V_o	Voltage applied on the focused acoustic ejector
f_{op}	Operation Frequency
f_{rep}	Repetition Frequency
$r_{1, 2, 3 \dots}$	Radii of the Annular Electrode
λ	Wavelength

Chapter 1 Introduction

1.1 Liquid ejections

1.1.1 Ejection modes

Continuous mode and drop-on-demand mode are the two common ejection modes in the printing process. Continuous ejection mode was introduced first in the early 1960s [Sweet, 1963]. The schematic diagram of a typical continuous mode ejection is shown in Fig. 1-1.

The pressure forces the ink to eject from the nozzle. The sinusoidal wave signal is applied to the nozzle, so the standing wave propagates along the ink jet and breaks the jet into drops of uniform size and spacing. The drops are continuously ejected. The discrete drops are then selectively charged by an instantaneous electric field. When passing through the pair of plates in which an electric field is developed, the charged drops are deflected to locate on the target substance. The uncharged drops are collected by the gutter.

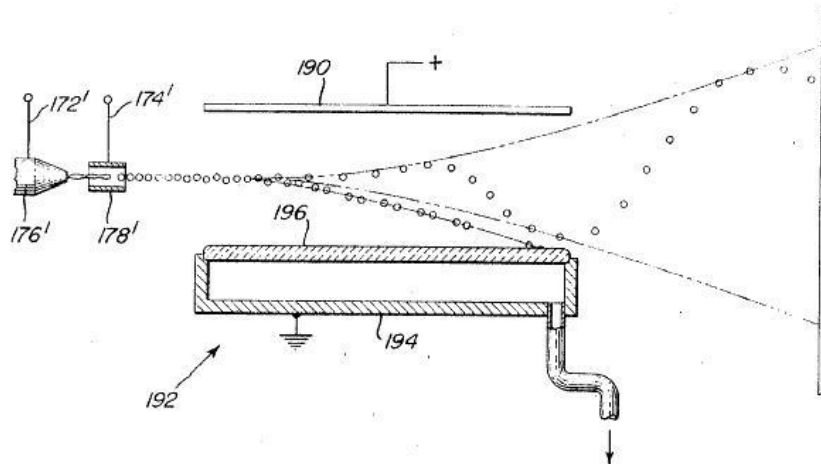




Fig. 1-1 Drawing of the first liquid ejector in continuous ejection mode [Sweet, 1963]

However, the continuous ejection mode was gradually abandoned and replaced by the drop-on-demand ejection mode. The drop-on-demand ejection mode was first introduced during the end of 1960s. The first drop-on-demand ejector was the electrostatic pull inkjet printer introduced during 1960s [Umezue et al., 2005]. The schematic diagram of a typical drop-on-demand ejector is shown in Fig. 1-2. A slight positive pressure is applied to ink such that a convex meniscus is formed. A high voltage electrode located on the outside of the nozzle is used to generate a pulse. The drops being charged by the electrode is ejected towards the target substance. With two orthogonal electrodes set on the substance, drops can be deflected in both vertical and horizontal directions, which is the drop-on-demand ejection mode.

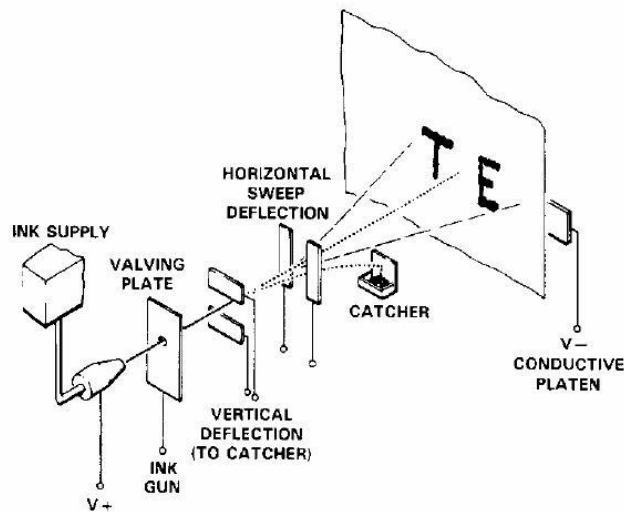


Fig. 1-2 Drawing of the electrostatic pull inkjet ejector, which was the first ejector in drop-on-demand mode

[Umezu et al., 2005]

There are several advantages of the drop-on-demand ejection mode over the continuous ejection mode. The ejection system can be greatly simplified by eliminating the charging electrode, the pair of electrostatic deflection plate, ink collection system and recirculation system. There is no need to use the complicated electronic circuit to select the drops to be charged. The drop-on-demand ejection mode only depends on the parameters relating to the actuation elements, assisting pressure control and the structure of orifice or nozzle. It also has potential to eliminate the adverse effect of ejecting liquid after recirculation process. In the conventional ejection, the liquid has to be pre-heated. The uncharged drops are re-circulated for next droplet ejection, but the liquid may change in properties,



which in turn change the ejection conditions such as applied voltage and pressure.

1.1.2 Ejection of viscous liquids

It has been suggested that the success of drop ejection is mainly related to the surface tension of the liquid [Elrod et al, 1989; Hadimioglu et al. 2001]. The surface tension is the reversible work as a result of the creation of a new surface area [Bicerano, 2002]. It is caused by the imbalance force acting on the molecules at the surface compared with the forces acting on molecules in the interior of a liquid. To form and expel a liquid drop from the surface, the surface tension of the liquid has to be overcome, e.g. by the pressure associated with the acoustic wave. However, it is also noted that before the formation of a drop, the liquid has to be deformed or stretched considerably. Therefore, viscosity which describes the internal resistance of the liquid to flow is also important and may even be more critical than the surface tension [Bicerano, 2002; Reis, 2005]. Viscosity is caused by the internal friction acting on a unit area in the direction opposite to the velocity gradient of the liquid. Because of the large resistance, high power is generally needed for the ejection of viscous liquids, which make the corresponding systems become large and complicated.

Viscous liquids are generally ejected by the drop-on-demand ejection mode. Common examples are the time-pressure ejection (dispensing), auger pump ejection, piston pump ejection and jetting. Mechanisms of these ejection methods are described as follows:

1.1.2.1 Contact mode ejection

In contact mode ejection is that during the ejection process, the liquid jets need to contact the target substrate at specific distance so as to obtain a consistent size of drops. If the distance between the needle and substrate is too short, the edge of the needle will be contaminated with the viscous liquid that increases the wetting area for drops' breaking off (Fig. 1-3a). If the distance is too long, the base area of liquid jet will be too small to contact the substrate for drop's breaking off. Both conditions result in the residue of liquid jets in the needle (Fig. 1-3b).

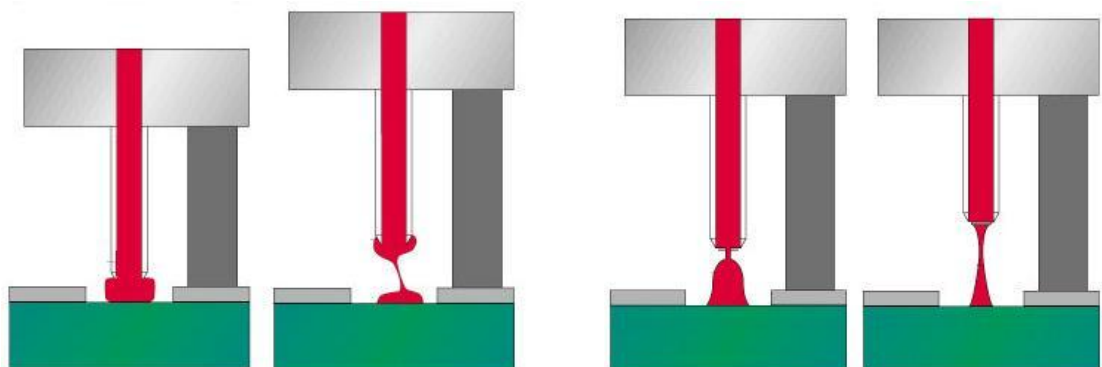


Fig. 1-3 Dispensing distance of contact mode ejection can cause inconsistent drops. (a) too short dispensing



distance (b) too long dispensing distance [Lewis et al. ,1999]

To obtain the desirable drops in the contact ejection mode, a z-directional control system is required. It monitors the distance and controls the displacement of the needle precisely for each droplet ejection, but its requirement becomes the major disadvantage of these ejection methods.

Three methods of contact mode ejection are describes as follows:

Time-pressure ejection

Fig. 1-4(a) shows the schematic diagram of the time-pressure ejection which is the most fundamental drop-on-demand mode ejection. The viscous liquid is simply pressurized and seeps out of a needle. The needle valve of the system is used to control the amount of viscous liquid to be ejected.

Auger pump ejection

The schematic diagram of the Auger pump ejection is shown in Fig. 1-4(b). The Auger feeding screw inserted in the liquid pipe can be switched on and off by a motor. The motor

makes the screw move vertically downward with a precise distance. In the mean time, the viscous liquid is sheared and the viscosity is decreased. The liquid is then forced out of the needle.

Piston pump ejection

The schematic diagram of a typical piston pump ejection system is shown in Fig. 1-4(c).

The piston is displaced by a certain distance. The viscous liquid is fed from the reservoir.

The displacement of the piston controls the amount of liquid to be ejected.

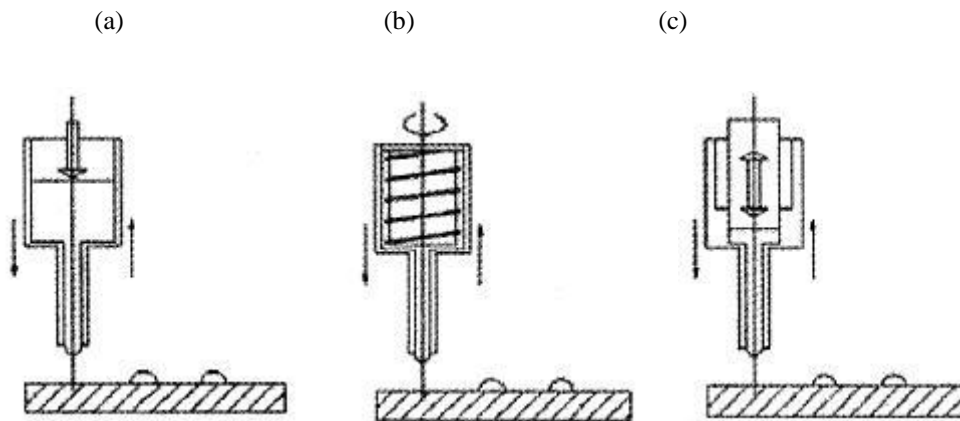


Fig. 1-4 Schematic diagrams of (a)Time pressure ejection (b)Auger pump ejection (c)Piston pump ejection

[Li et al. ,2004]



1.1.2.2 Non-contact mode ejection

Asymtak Company and Mushashi Engineering Inc. have investigated the non-contact mode ejection since 1990s [Li et al., 2004]. During the ejection process, the needle with liquid jet is located at a distance from the substrate. The drops are ejected and travel to the target substrate. A typical example of non-contact mode ejection is Jetting, which was introduced by Asymtak Company.

Jetting

The schematic diagram of a typical jetting system is shown in Fig. 1-5 [Li et al., 2004; Piracci, 2000]. The liquid is pressurized to fill the entire system. The chamber and the liquid path are preheated for decreasing the viscosity of the liquid. Ball and seat design are stored in the liquid path. When the ball retracts from the seat, the viscous liquid fills the space. When returning, the liquid is accelerated toward the orifice. Due to the shear, the viscosity of the liquid is reduced and the drops are ejected.

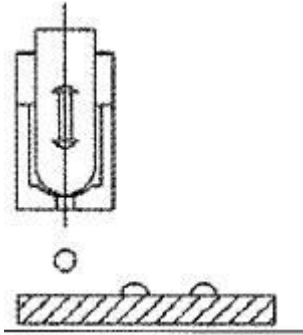


Fig. 1-5 Schematic diagram of Jetting dispensing [Li et al., 2004]

Jetting which utilizes the non-contact ejection mode can eliminate the z-directional control system. The control system for ejection can be simplified. However, the jetting system including the pressure control and long actuator is too large and heavy. The movement of the printhead for ejection is difficult and inconvenience.

1.2 Piezoelectric ejection

1.2.1 Mechanisms of piezoelectric ejectors

Piezoelectric ejection was first developed in 1970s, and recently becomes the dominant ejection method in the ejection/printing industries. Many researchers have put a lot of efforts on the calculation of the ejection parameters. The structure of the ejector, including the nozzle, transducer and pressure system, has been investigated and modified.



There are two major mechanisms of the piezoelectric ejectors. One of them utilizes the displacement generated by piezoelectric materials to cause a volume change in the liquid chamber for drop ejection. The other mechanism utilizes the acoustic wave generated by piezoelectric materials to vibrate a membrane and hence to generate a capillary wave at the orifice for ejecting liquid drops.

Piezoelectric material has a property of conversion of the electrical driving voltage into a mechanical deformation. (A detailed introduction of the piezoelectric effect and piezoelectric materials will be given in Section 1.4) The deformation of the piezoelectric material generates an actuating force to deform the liquid chamber. The pressure change inside the chamber makes the liquid eject from the nozzle to form a drop. There are various modes of operations, such as squeeze mode, bend mode and push mode, for piezoelectric ejectors.

Squeeze mode: Piezoelectric ejector utilizing the squeeze mode was first introduced as a liquid ejector by Zoltan of the Clevite Company in 1970s. Fig. 1-6 shows the schematic diagram of a typical squeeze-mode piezoelectric ejector [Zoltan et al., 1970]. A

cylindrical tube of a piezoelectric material is inserted in a cylindrical ink chamber. When a voltage is applied, the piezoelectric material deforms in the radial mode. The chamber is then squeezed and a drop of liquid is ejected. The change of volume in the chamber is equal to the volume of the ejected drop.

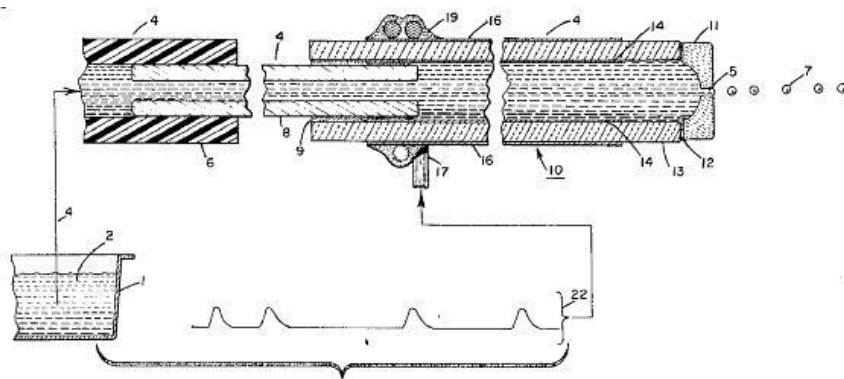


Fig. 1-6 Drawing of the first piezoelectric ejector deforms in squeeze mode. [Zoltan et al., 1970]

Bend mode: Fig. 1-7 shows the schematic diagram of a typical bend-mode piezoelectric ejector [Stemme, 1972]. A piezoelectric disc is attached at the back of a liquid chamber. When a voltage is applied, the piezoelectric disc vibrates at the thickness resonances mode. As a result of the Poisson contraction, the diaphragm vibrates to change the volume of the liquid chamber, and hence a drop of liquid is ejected.

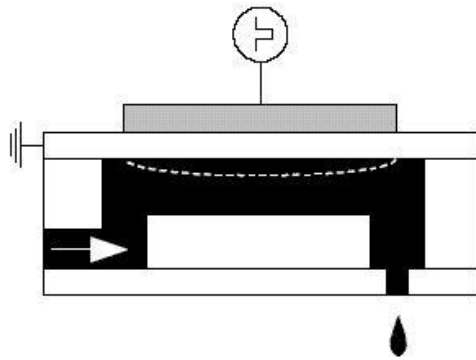


Fig. 1-7 Schematic diagram of the piezoelectric ejector deforms in bend mode

Push mode: Fig. 1-8 shows the schematic diagram of a typical push-mode piezoelectric ejector [Howkins, 1982]. A piezoelectric bar is attached at the back of a liquid chamber and above an orifice or nozzle. When a voltage is applied, the piezoelectric bar vibrates at the length resonance mode. As a result, the volume of the liquid chamber changes and a drop of liquid is ejected.

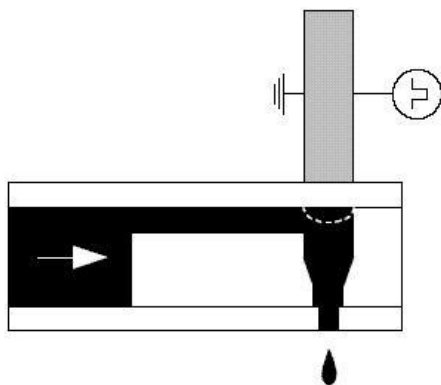


Fig. 1-8 Schematic diagram of the piezoelectric ejector deforms in push mode



An alternative mechanism of liquid ejection using piezoelectric materials was introduced in the last decade. Instead of the piezoelectric displacement, the ultrasonic waves generated by a piezoelectric material are utilized to vibrate a thin membrane. The resulting vibration then develops a capillary wave at the liquid-air interface at the orifice [Percin, 2003; Demirci et al., 2005]. It increases the pressure without pressing the liquid (including atmosphere pressure). When the pressure is high enough to overcome the inertia and surface tension of the liquid, drops are ejected from the orifice.

Fig. 1-9 shows the schematic diagram of a typical piezoelectric ejector utilizing the ultrasonic waves [Lam et al., 2004; Wang et al., 2007]. A piezoelectric annular disc is bonded to a thin metal diaphragm with a small orifice. The compound plate is then attached to a cylinder which serves both as a liquid reservoir and to clamp the ends of the plate. The reservoir is open and the liquid is at atmosphere pressure. When a voltage is applied, the plate vibrates at its resonance frequency, giving a maximum vibration at its center. The liquid behind the orifice is accelerated as the plate moves. When the inertial force is larger than the surface tension, a drop is ejected from the orifice.

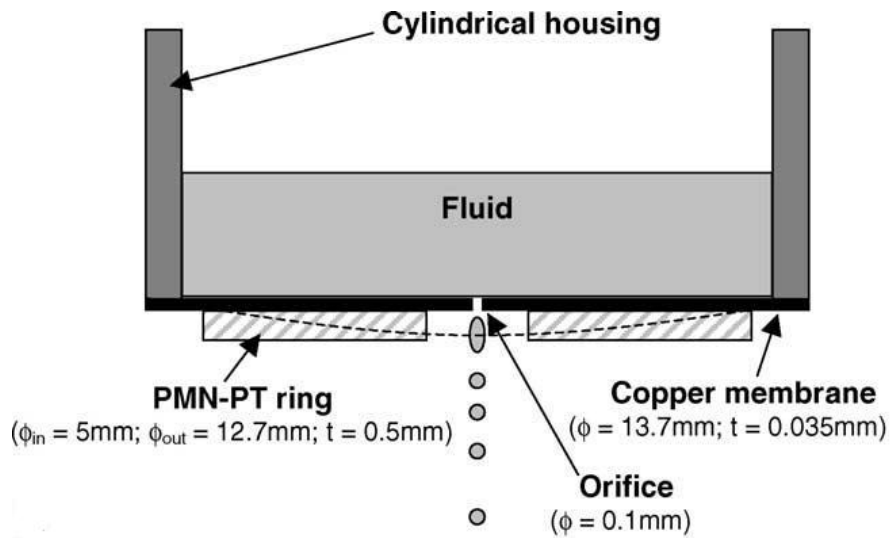


Fig. 1-9 Schematic diagram of the piezoelectric annular ejector which utilizes the ultrasonic wave to vibrate the copper membrane [Lam et al., 2004]

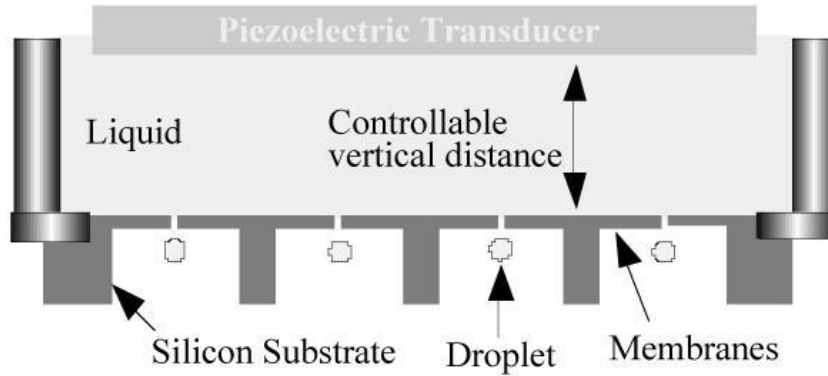


Fig. 1-10 Schematic diagram of the piezoelectric ejector utilizing ultrasonic wave to eject the drops [Demirci et al., 2006]

Fig. 1-10 shows the schematic diagram of the piezoelectric ejector developed by Demirci et al. [2006]. A piezoelectric transducer is placed coaxially at a distance with membrane



which composes of multiple orifices. When a voltage is applied to the transducer, ultrasonic waves are generated, actuating the membrane to eject multiple drops from the orifice.

1.2.2 Advantages of piezoelectric ejectors

All piezoelectric ejectors are operated in the drop-on-demand and non-contact ejection mode, so the ejection system and ejection control system can be simplified as discussed in previous sections. The ejector has a simple electronic circuit which consists of a signal generator, a power amplifier, and the ejector connected in series. The pressure control system is also simple because only a constant pressure is generally required. Therefore, the piezoelectric ejector can be small in size.

1.2.3 Ejection of various liquids

Applications for liquid ejection are rapidly expanding. The ejectors are required to eject not only ink for imaging or printing, but also other liquids in various industries. For examples, the ejectors have been used to eject the luminescence liquid for manufacturing Liquid Crystal Display (LCD). The ejection of polymer is used for making a micro lenses in optical technology. In chemical experiments, the drop ejection is applied for mixing



precisely two chemicals with solvents and for delivering drugs [Lee et al., 2006]. In biological industries and life science markets, the drop ejection is applied for DNA spotting, cell sorting and protein substances ejection [Pickett et al., 2006]. The ejection of viscous liquids is also important for various industries. However, because of the weak piezoelectric force or small piezoelectric displacement, it is generally difficult for the conventional piezoelectric ejectors to eject viscous liquids unless the liquids are preheated to high temperatures [Hayes et al., 1998]. In this work, we aim at studying the ejection of viscous liquids using focused acoustic wave which is generated by piezoelectric materials. It is expected that the enhanced acoustic wave intensity is high enough to stretch and then eject the viscous liquids.

A small nozzle is generally required in most of the piezoelectric ejectors for ejecting liquid drops. However, the small nozzle is difficult to construct with good uniformity, and is susceptible to clogging. In ejecting viscous liquids as well as volatile liquids with suspended particles, the clogging problem becomes more severe [Lee, 2002]. Due to the evaporation, the viscosity of the volatile liquids will increase during the process and solid residues are even formed. The viscous liquids will block the aperture or part of the aperture of the nozzle. The asymmetric nozzle causes misdirected drop and inconsistent



droplet size, which are not allowed for practical applications and hence have to be remedied. Therefore, nozzleless ejection is desired, in particular for applications involving viscous liquids.

1.3 Focused acoustic ejection

1.3.1 Focused acoustic ejectors

In 1979, Lovelady et al. [1979] discovered that the curved transducers immersed in the liquid could generate synchronous drops and fog (Fig. 1-11a). They suggested that the acoustic wave generated by the piezoelectric material was able to provide a pressure at the liquid-air interface. The pressure could make the liquid surface unstable and form several drops simultaneously.

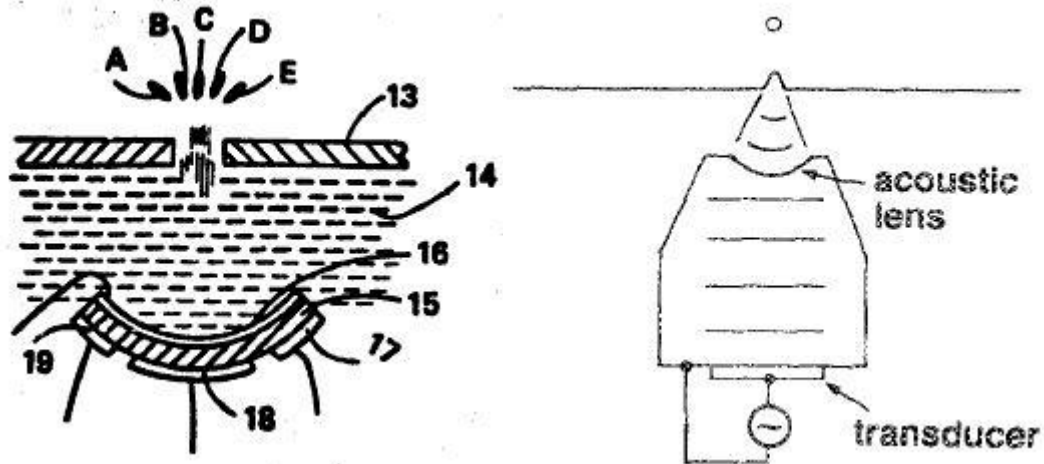


Fig. 1-11 Drawings of (a) the curved transducer generated several drops simultaneously [Lovelady et al. 1979] and (b) the focused acoustic ejector composed of acoustic lens and transducer [Elrod et al., 1989].

In 1988, S. A. Elrod showed that a focused acoustic wave was capable of ejecting liquid drops from the surface of liquid without a nozzle in the drop-on-demand mode (Fig. 1-11b). Focused acoustic ejectors contain two main components: acoustic transducer and focusing element [Elrod et al., 1989; Hadimioglu et al., 1992; Ellson et al. 2003; Amemiya et al., 2007]. The ejectors are able to focus the acoustic waves at the liquid surface for drop ejection. One end of the acoustic transducer (usually actuated by a piezoelectric material) is bonded to a rigid surface and the other side is attached to the focusing element (Fig. 1-11b). There are a number of focusing elements, such as spherical acoustic lens and Fresnel acoustic lens. When a voltage is applied to the transducer,



acoustic waves are generated and propagated along the focusing element to converge at the focal point. The liquid level is adjusted such that the converging acoustic waves focus at the liquid surface. The acoustic waves are confined to the dimension of focal point whose size is related to the wavelength of the acoustic waves. Radiation pressure associated with the acoustic waves make the liquid surface deforms [Elrod et al., 1989]. When the acoustic pressure is large enough to overcome the surface tension of the liquid, a drop is ejected from the liquid surface.

Besides the acoustic wavelength, the size of the drops produced by the focused acoustic ejection can be adjusted by the liquid level which changes the dimension of the focal point [Elrod et al., 1989; Huang et al., 2001]. Hence, a precise system for controlling the liquid level is needed for consistent drop ejection. Sonar measurement system has been equipped in some of the commercial acoustic ejectors. A short pulse of acoustic energy is generated and the time for the pulse traveling towards and backwards from the liquid surface is recorded. The liquid level can be calculated with a known sound speed in the liquid. Accordingly, the transducer can be located at the designed liquid level (e.g. focal length).



The use of focused acoustic waves to actuate drop ejection was invented and developed at Xerox PARC in 1980s. The company holds over a hundred patents relating to this innovative ejection technique. Commercial focused acoustic ejection systems are developed by a number of printing companies, such as EDC Biosystem, Picoliter and Laycyte. Fig. 1-12 (a) shows Acoustic Transfer System ATS-100 introduced by EDC Biosystem. The system includes a pulse-echo system to determine the focal length for consistent drop ejection [Forbush]. Fig. 1-12 (b) shows Portail 630 Reagent multi-spotter designed by Laycyte, which can deposit a sub-nanoliter drop of low-viscosity liquid precisely [Pickett et al., 2006]. Fig. 1-12 (c) shows an acoustic multi-ejector printhead fabricated by Xerox PARC, which can print photo-quality image at room temperature [Hadimioglu et al., 2001]. The acoustic spherical lens is used as their focusing element in the above ejection systems.

(a)

**ATS-100**

(b)



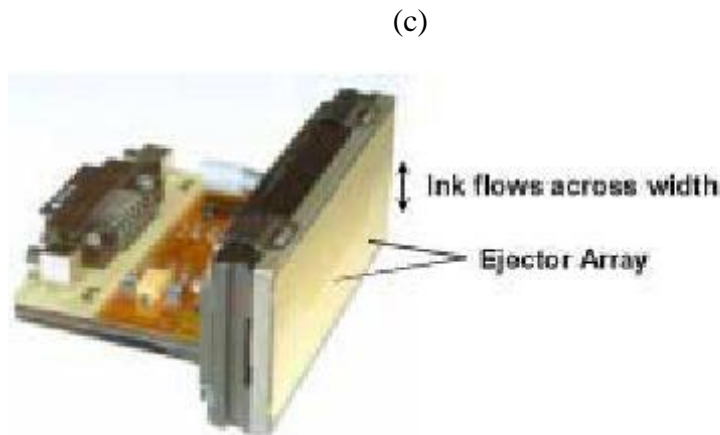


Fig. 1-12 The commercial focused acoustic ejectors: (a) ATS-100 [Forbush, EDC Biosystem] (b) Portail 630 Reagent multi-spotter [Pickett et al. 2006] (c) acoustic multi ejector printhead [Hadimioglu et al., 2001]

1.3.2 Focusing elements

1.3.2.1 Physical lens and its focusing mechanism

Typical examples of physical lens are spherical lenses and Fresnel acoustic lenses. The spherical lens has a semispherical geometry. It can be fabricated by polishing and grinding. A smaller spherical lens can be fabricated by the ejection of small polymer drops on the substance. On the other hand, Fig. 1-13 shows Fresnel acoustic lens which has planar structure. The small Fresnel acoustic lens can be fabricated by depositing a layer of silicone and etching the layer to form the pattern.

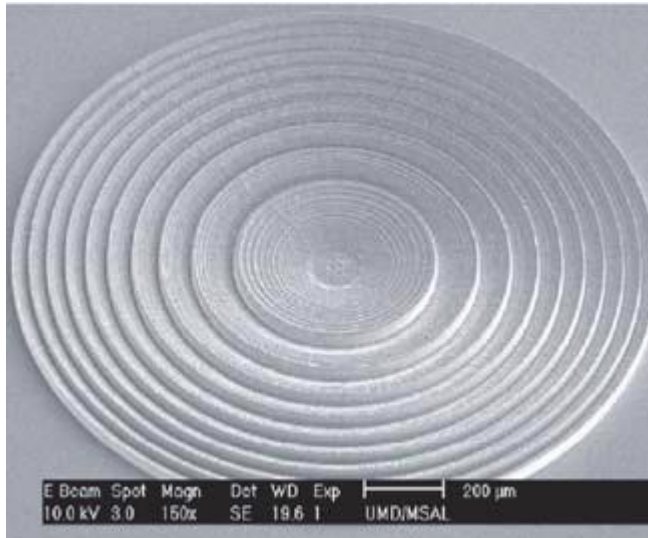


Fig. 1-13 SEM diagram of Fresnel (phase) acoustic lens fabricated by reactive ion etching [Milster, 2009]

The mechanism of focusing by physical lens is that the acoustic waves received from the transducer propagate along the lens. The acoustic waves then refract toward the focal point.

1.3.2.2 Lensless focusing and its focusing mechanism

Typical examples for the lensless focusing elements are the phased delayed system and Fresnel zone plate (FZP). Phased delayed system shown in Fig. 1-14 [Kino, 2001; Kawanami, 2001] consists of a series of individual transducer elements. Each of them can

be excited by a voltage separately and hence generates acoustic waves at different times, i.e. the phases of the acoustic waves have are different. As a result, the wavefront of the resultant outgoing waves will changes from a plane form to other forms, depending on the phase difference between the individual waves. For focusing purpose, the elements located in the central part will be excited at a later time, i.e. delayed, and the focal length is controlled by the amount of delay.

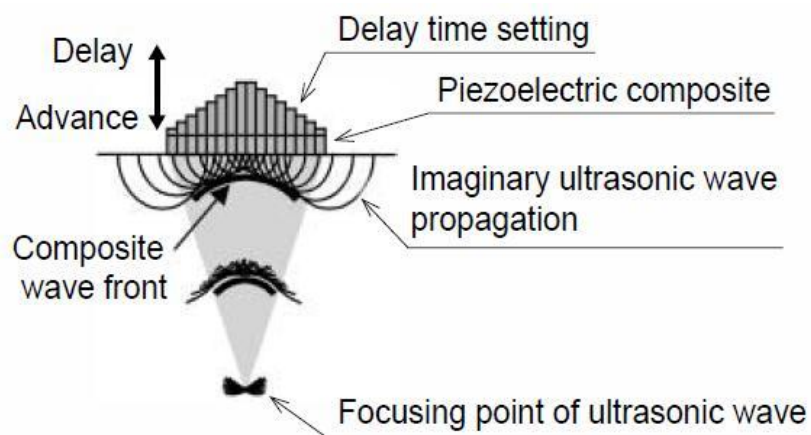


Fig. 1-14 Schematic diagram of phased delayed system [Kawanami, 2001]

1.3.2.2.1 Fresnel zone plate

Augustin-Jean Fresnel discovered that the irradiance behind a circular aperture illuminated with a uniform laser beam exhibit bright concentric rings pattern which were

called Fresnel zones. In 1875, Soret constructed the first FZP consisting of alternative transparent and opaque annular plate originated from the Fresnel zone principle [Hristov, 2002]. Fig. 1-15 shows the conventional FZP is a metal plate with a number of circular apertures which allow part of the illuminated light to pass through. The other part, i.e. the "opaque" region, blocks the light to pass through.

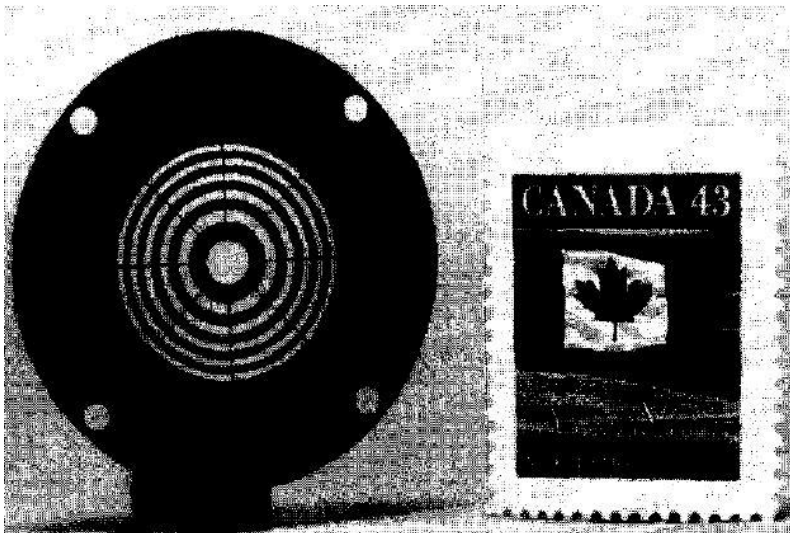


Fig. 1-15 Photograph of the stainless steel micro-machined FZP for ultrasonic focusing [Schindel, 1997]

The focusing mechanism of the FZP is also related to phase difference. According to Huygens' Principle, the aperture acts as a secondary spherical wave source. Constructive interference occurs at the observation point where the path difference equals an integral number of the wavelength λ . Destructive interference occurs at the observation point



where the path difference equals $(m+1/2)\lambda$, where m is an integer. Each circular aperture in the plate is a Fresnel zone, which corresponds to successive increments of $\lambda/2$ in path difference. As a result, only constructive interference (or destructive interference) occurs at the observation point, giving a significant enhancement in intensity. In other words, the waves self-focus at the observation point or focal point.

The self-focusing phenomenon can also be realized in acoustic waves. The "transparent" Fresnel zones is transferred and replaced by a series of annular electrodes on a piezoelectric plate. The acoustic waves generated by the electrodes are equivalent to the light passing through the "transparent zone". Similarly, the acoustic waves will self-focus at the focal point because of the constructive interference.

Huang et al. [2001] has successfully utilized the FZP in fabricating micro-machined self-focused acoustic ejectors. The Al-ZnO-Al sandwich structure was supported by a low stress silicon-nitride diaphragm as shown in Fig. 1-16 [Huang et al., 2001]. The Al electrodes were patterned in the form of FZP. They showed that, because of the self-focused acoustic waves generated by ZnO, water drops were ejected from the water surface in the drop-on-demand mode.

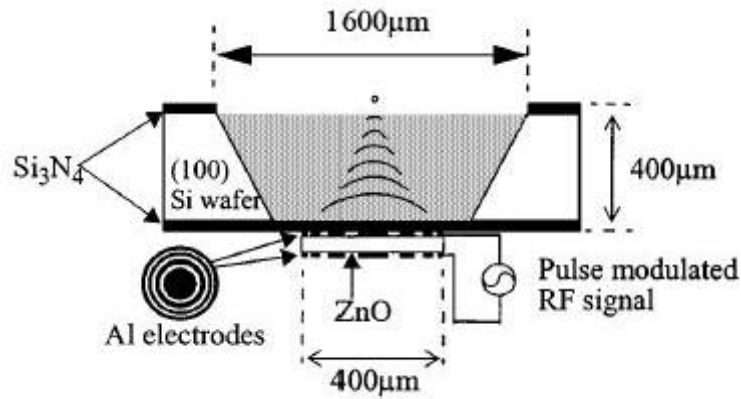


Fig. 1-16 Schematic diagram of the micromachined self-focused acoustic ejector with ZnO FZP [Huang et al., 2001]

Kwon et al. demonstrated a directional drop ejection by using an "incomplete" FZP [Kwon et al., 2002; Lee et al., 2006]. As shown in Fig. 1-17, a sector of the annular electrodes was carved out from a "complete" FZP, and due to the asymmetric vibrations, the drops were ejected at some deflection angle.

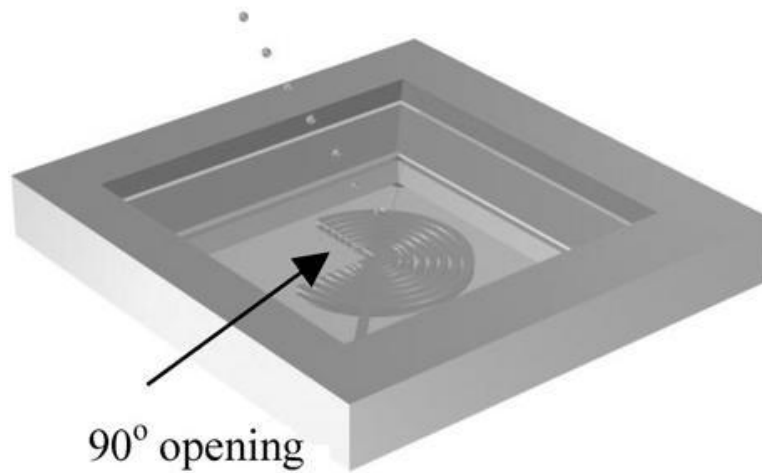


Fig. 1-17 Diagram of the “Incomplete” FZP for directional drop ejection [Kwon et al., 2002]

By using a similar structure of Huang et al., Yu et al. developed a device for ejecting oil drops from an oil-water composite liquid as shown in Fig. 1-18 [Yu et al., 2005]. Instead of ZnO, PZT piezoelectric ceramic sheet was used in their work for the FZP.

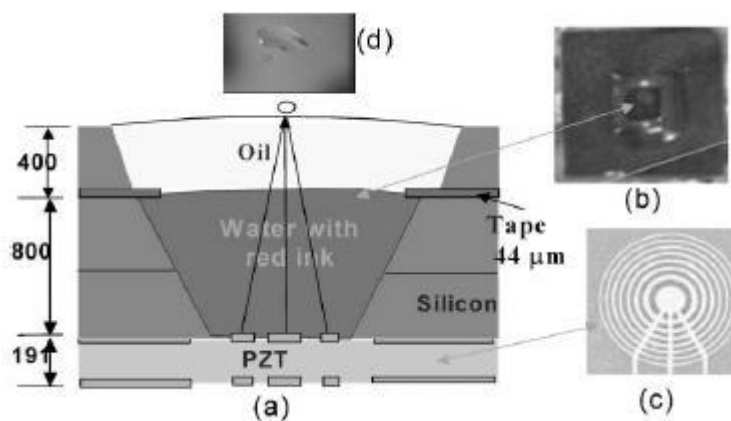


Fig. 1-18 Schematic diagram of self-focused acoustic ejector ejecting oil drops from oil-water composite

liquid [Yu et al., 2005]

Lee et al. [2006] developed a novel FZP with air reflectors. Air pockets patterned by a Parylene layer were fabricated on an electroded PZT piezoelectric plate. Fig. 1-19 shows the schematic diagram of self-focused acoustic ejector employing air reflector. The air reflectors acted as the air reflectors to block part of the acoustic waves generated by the PZT piezoelectric plate. As a result, only the acoustic waves generated in the "transparent" Fresnel zones could transmit, propagate, constructively interfere and hence self-focus in the liquid. The novel structure increased the acoustic wave amplitude, in particular for those generated from the outer region, and hence improved the performance of the ejection.

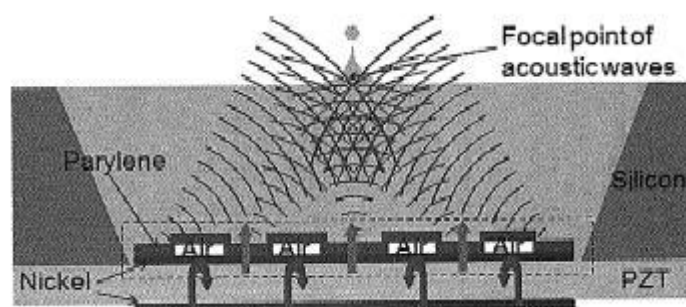


Fig. 1-19 Schematic diagram of the self-focused acoustic ejector employing air reflector which blocks the propagation of part of acoustic wave for self-focusing [Lee et al., 2006]

Lee et al. [2008] employed the higher harmonic resonances of the PZT piezoelectric plate in their self-focused acoustic ejector as shown in Fig. 1-20. Due to the increase in the operation frequency of the piezoelectric plate, the wavelength of the acoustic wave in the liquid decreased and hence the diameter of the drops decreased.

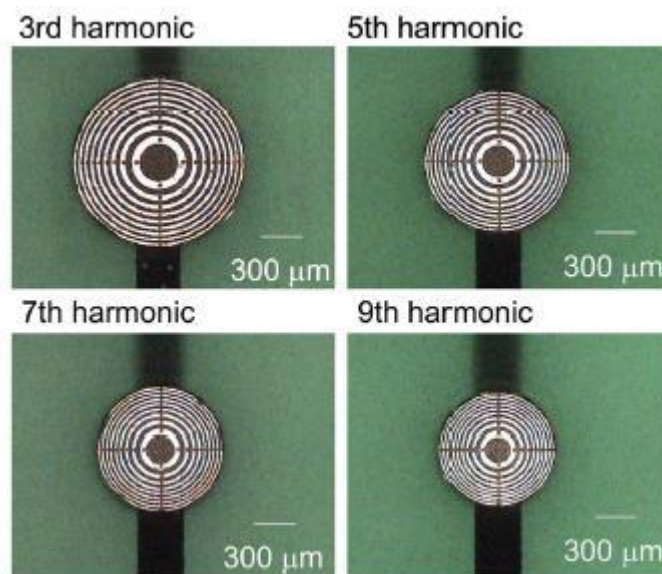


Fig. 1-20 Photograph of the self-focused acoustic ejectors designed for different harmonic frequencies to generate smaller drops [Lee et al., 2008]

Table 1-2 summarizes the performances and operation conditions of the focused acoustic ejectors fabricated using the Fresnel zone plates. It can be seen that liquids with a low



viscosity, such as water, are usually used for the demonstration of the ejection. In this work, we aim at design and fabricate focused acoustic ejectors using the Fresnel zone plates as the focusing element for the ejection of viscous liquids.

1.3.3 Advantages of Focused acoustic ejection

One of the major advantages of focused acoustic ejection is the capability of ejecting biological liquids or liquids with particulates. Examples are DNA, proteins, living cells etc. The conventional piezoelectric ejectors cannot be used to eject these liquids. The ejection capability of the piezoelectric ejectors strongly depends on the size and structure of the nozzle. Due to the small nozzle, misdirected ejection, inconsistent drop size and even clogging usually occur. Unlike the piezoelectric ejectors, the focused acoustic ejectors can eject liquid drops with a large orifice or even nozzleless. The large orifice allows the particulates to pass through, hence clogging will not occur. The droplet size is independent of the dimensions of the orifice, so tiny drops can be ejected.

It is anticipated that the focused acoustic ejectors can be used to eject viscous liquids. Due to its nozzleless structure, the clogging problem does not exist. If the pulse energy is large enough to overcome the surface tension of the viscous liquids, the drop ejection can be



done. Amemiya et al. [2007] have demonstrated that resin with a viscosity of about 400 cP (for light emitting diode packaging) can be ejected using focused acoustic ejectors. Therefore, it is of interest to investigate the ejection of viscous liquids (with viscosity larger than 1000 cP) by focused acoustic ejectors.

The focused acoustic ejection is classified as a non-contact mode ejection which has several advantages over the contact mode ejection. The positioning system for the non-contact mode ejection can be simplified. As there is no z-directional control, the ejection rate can be enhanced.

As mentioned before, the size of the drops produced by the focused acoustic ejector can be adjusted by the liquid level which changes the dimension of the focal point. Sonar measurement system has been equipped to adjust the position of transducer according to the liquid level. In the upward ejection, it is important to determine the liquid level. Our experiment, in the downward ejection, this system is not required. The volume of the reservoir is fixed and so refilled entirely the reservoir, the consistent drops can also be obtained.



1.4 Piezoelectricity

Fig. 1-21 shows a poled piezoelectric ceramics have inverse piezoelectric effect between electric energy and mechanical energy. The converse piezoelectric effect is the linear and reversible strains generated in the piezoelectric ceramics in the response of an applied voltage. The deformation of the poled piezoelectric ceramics depends on the polarity of applied voltage and the polarization of the ceramics. As illustrated in Fig. 1-21(a), when the applied voltage has same polarity as polarization of the plates, the plates will lengthen. When the applied voltage has polarity opposite to the polarization of the plates, the plates will shorten. Hence, if an alternating voltage at certain frequency is applied, the ceramics deforms cyclically at the same frequency. On the other hand, the direct piezoelectric effect is the opposite phenomenon in which mechanical compression or tension on the poled piezoelectric ceramics changes the dipole moments, generating a voltage as illustrated in Fig. 1-21(b). The voltage of same polarity is generated when the compression along the direction of polarization or tension perpendicular to the direction polarization is applied.

The principle of converse piezoelectric effect is adapted to the piezoelectric transducer

such as motor and sound generator. Acoustic wave of the self-focused acoustic ejector is generated by the mechanical actuation of piezoelectric material in the liquid. On the other hand, the principle of direct piezoelectric effect is applied to the piezoelectric sensor such as force sensor and ultrasonic scanning.

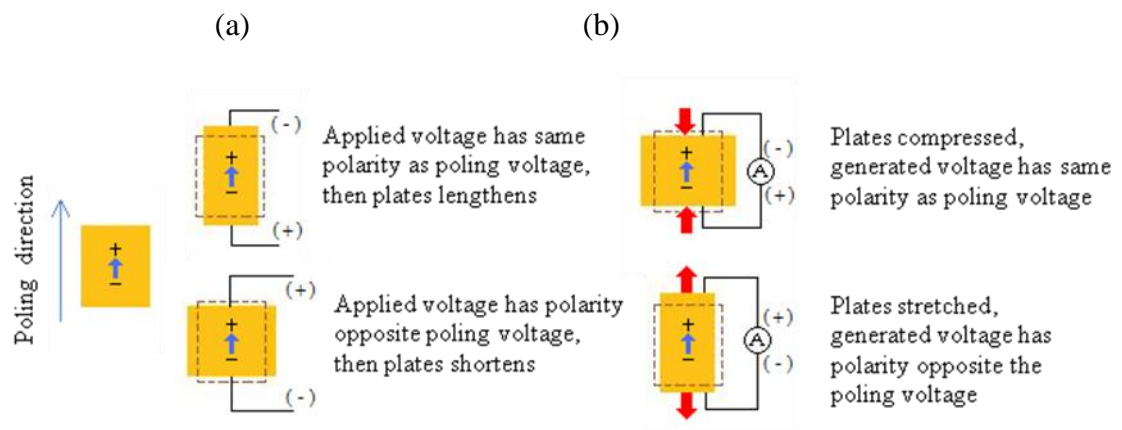


Fig. 1-21 (a) Converse piezoelectric effect and (b) direct piezoelectric effect of piezoelectric material

PZT ($\text{Pb}(\text{Zr}_x\text{Ti}_{1-x})\text{O}_3$) [Kwon et al., 2004], ZnO [Huang et al., 2001], LiNbO_3 [Percin, 2003] and PMN-PT ($\text{Pb}(\text{Mg}_x\text{Nb}_{1-x})\text{O}_3\text{-PbTiO}_3$) [Lam et al., 2005] have been used as the actuating element of piezoelectric ejectors. Among the piezoelectric materials, PZT is most commonly employed for smart material application at present and is widely used commercial industry.

With different dopants, hard PZTs and soft PZTs are fabricated for suiting the different



applications. Soft PZTs usually have a larger electromechanical coupling factor than hard PZT, indicating the production of larger displacement. However, soft PZTs usually have higher dielectric loss, so it cannot be applied a high voltage during actuation. Therefore, soft PZTs are usually used in the sensing applications. Hard PZTs have opposite characteristics of higher stability, higher mechanical quality factor, difficult to be depolarized. Hard PZTs are compatible with high mechanical loads and high voltages, so they are usually used in the actuating applications. Therefore, for the self-focused acoustic ejector, hard PZT (America piezo 880) was used. It is usually used for ultrasonic mixing and dispensing applications. Table 1-1 shows the physical and piezoelectric properties of piezoelectric material APC 880.

Table 1-1 Physical and piezoelectric properties of piezoelectric material APC 880

Relative Dielectric Constant		Dielectric Loss (%)		Density (g/cm ³)		Curie Point (°C)	
1000		0.35		7.6		310	
Electromechanical Coupling Factor (%)		Piezoelectric Charge Constant (x10 ⁻¹² C/N)		Piezoelectric Charge Constant (x10 ⁻³ Vm/N)			
k _p	0.5	d ₃₃	215	g ₃₃	25		
k ₃₃	0.62	-d ₃₁	95	-g ₃₁	10		



k_{31}	0.30	d_{15}	330	g_{15}	28
k_{15}	0.55				
Young Modulus (GN/m ²)		Frequency Constant (Thickness) (MHz/mm)		Mechanical Quality Factor	
72		2.210		1000	

1.5 Scope of work

The main objective of the present work is to study self-focused piezoelectric transducers for ejecting drops of high-viscosity liquid, without nozzle, in the drop-on-demand mode. Focused acoustic ejector using the self-focused piezoelectric transducers will be designed and fabricated, and their ejection performances then evaluated.

Instead of using focusing elements, self-focused piezoelectric transducer based on the FZP will be designed and fabricated as the driving element for the ejector. “Milled” FZP will be utilized in an attempt to reduce the hindrance of un-excited part of piezoelectric material. Their theory, design and fabrication are described in Chapter Two.

The capability of self-focusing, including the distribution of the wave intensity and locations of the focal points are important factors in the performances of the ejector. A



needle-type hydrophone will be used to measure the wave intensity in the liquid for this purpose. The intensity distributions for non-milled and milled FZPs will be used to assess the effects arisen from hindrance. Their measurements, results and comparisons are discussed in Chapter Three.

The fabrication and performance evaluations of the ejectors are described in Chapters Four and Five. Different viscous liquids, such as glycerin (1400 cP), pre-polymers of epoxy (~ 2000 cP) and domestic detergent will be used for the evaluation. The effects of the operation parameters, including the amplitude and duration of the driving voltage, the repetition frequency, liquid level and the operation frequency of the transducer, will be investigated. On the basis of the results, the optimum operation parameters will be determined.



Table 1-2 Summary of the ejection conditions and performances of self-focused acoustic ejector

	Piezoelectric Material (Dimension)	Operation Frequency (MHz)	Focal Length (μm)	Liquid Used (viscosity)	Pulse Duration	Maximum Repetition Frequency (Hz)	Driven Pulse Amplitude (V)	Droplet Size (μm)
Huang (2001)	ZnO thin film (400 μm)	600	350	Water (1 cP)	5 μs	>10 000	nil	5
Yu (2004)	PZT sheet (191 μm)	10.8	3	Water (1 cP)	25 μs	500	86	100-300
				Isopropanol (4 cP)	20 μs	1100	86	110
				Oil (55 cSt)	40 μs	40	86	220
Lee (2006)	PZT sheet (127 μm)	18	800	Water (1 cP)	7 μs	10000	60	70
Lee (2008)	PZT sheet (127 μm)	20	800	Water (1 cP)	8 μs	120	70	80

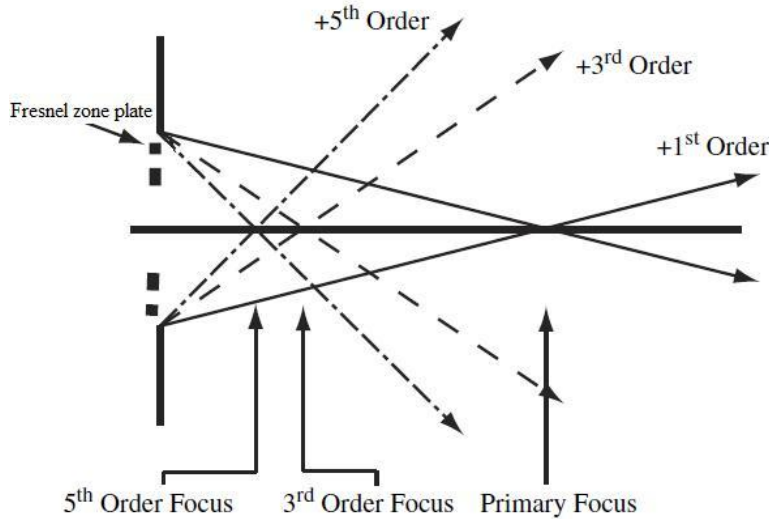


Chapter 2 Design and Fabrication of the Fresnel Zone Plates

Hemispherical lenses are commonly used as the focusing elements in commercial acoustic ejectors. However, the fabrication of the lenses is difficult and costly. The lenses must be polished precisely to give an unevenness of the spherical surface smaller than $1/10$ of the acoustic wavelength [Kanda, 1980]. The diameter of the aperture should not be too large compared to the focal length so as to eliminate the spherical aberrations. The processes of mechanical grinding and polishing are time-consuming and expensive. Moreover, the selection of materials for the lens is also restricted by a number of considerations, such as the acoustic velocities of the liquid, refractive index of the materials and the impedance between liquids and lens. Silica, quartz and glassy carbon are generally used for the lenses.

As compared to the spherical lenses, phased delayed system is preferable because of the simple structure and easy fabrication. However, the corresponding electronic control system is relatively complicated. Each piezoelectric element has to be excited separately. On the other hand, the Fresnel zone plate has both converging and diverging properties with multi-foci (illustrated in Fig. 2-1) as well as the simple electronic circuit. The planar structure of the zone plate is another advantage making the fabrication of the plate easier and cost effective. Therefore, the Fresnel zone plate (FZP) is selected in this work as the focusing element for the focused acoustic ejectors.

(a)



(b)

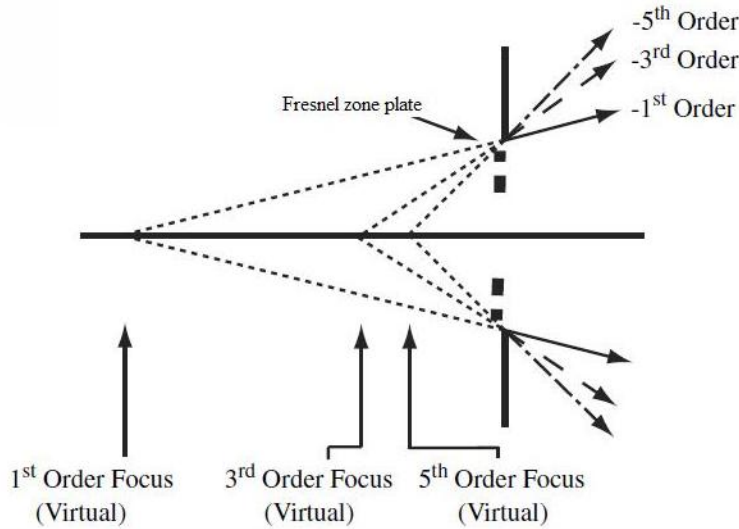


Fig. 2-1(a) Converging and (b) diverging properties with multi-foci of FZP [Milster, 2009]

2.1 Design of the Fresnel zone plate

2.1.1 Theory

As mentioned in Chapter 1, for acoustic wave applications, the FZP consists of a series of annular electrodes patterned on a piezoelectric plate as shown in Fig. 2-2. The inner and outer radii of each annular electrode (i.e. Fresnel zone) are denoted by r_{2k} and r_{2k+1} , respectively with k is integer starting from 0. The acoustic waves from each zone (i.e. generated by the piezoelectric plate at the annular electrode) will propagate,

constructively interfere and then self-focus in the liquid.

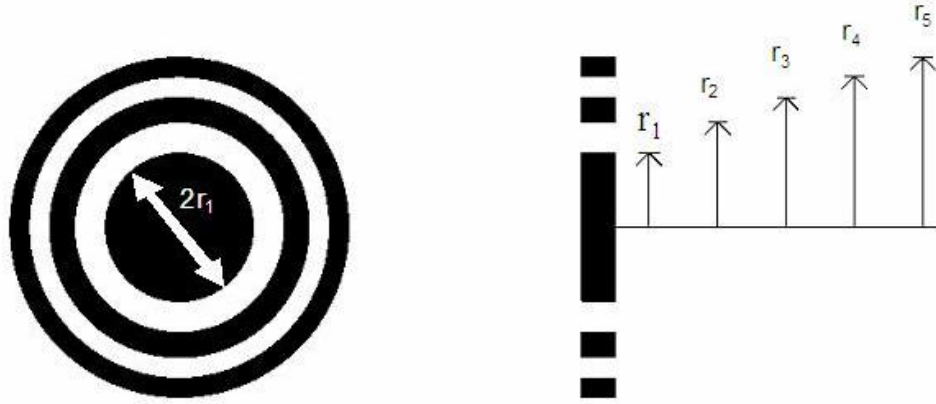


Fig. 2-2 The FZP patterned on the piezoelectric plate to self-focus the acoustic waves

Assume that the designed focal point is F_d and the corresponding focal length is L_d . As all the waves when arrive at F_d are in-phase and constructively interfere with each other, the wave generated at a particular point of an annular electrode should have a path difference of an integral number of the wavelength from the wave generated at a corresponding point of the adjacent electrode (see Fig. 2-3):

$$R_{i+2} - R_i = m\lambda \quad (2-1)$$

where m is an integer and λ is the acoustic wavelength in liquid. Destructive interference between the waves generated at the same annular electrode should be minimized. Hence, the path difference between the waves generated at the edges of an annular electrode should satisfy (see Fig. 2-3):

$$R_{i+1} - R_i = \frac{\lambda}{2} \quad (2-2)$$

In order to fulfill both the conditions (Eq. 2-1 and Eq. 2-2), m is taken as 1. The radii r_n of the annular electrodes in Fig. 2-2 are then given as:

$$r_n = \sqrt{n\lambda L_d + \left(\frac{n\lambda}{2}\right)^2} \quad (2-3)$$

where $n = 1, 2, 3 \dots$

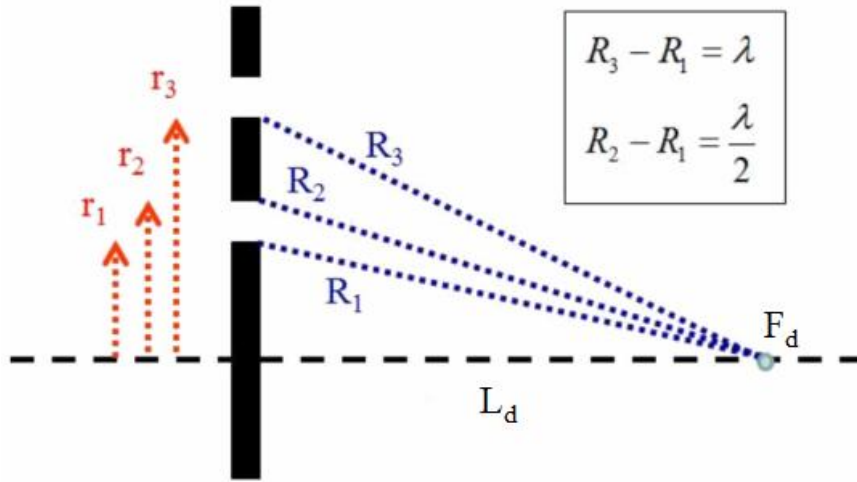


Fig. 2-3 Effect of path difference on wave interference with FZP

2.1.2 The Fresnel approximation

As mentioned in Chapter 1, the FZP was firstly developed for optical applications. In those applications, the inner and outer radii of each Fresnel zone (i.e. the annular electrode in the FZP in Fig. 2-2) are given as [Ersoy, 2007; Milster, 2009]:

$$r_n = \sqrt{n\lambda L_d} \quad (2-4)$$

It is noted that Eq. 2-4 can be obtained from Eq. 2-3 if an approximation of $L_d \gg \lambda$ is taken. There is no assumption or approximation used in deriving Eq. 2-3. In fact, the approximation of $L_d \gg \lambda$ is part of the Fresnel approximations: $R \gg \lambda$ and $2r \gg \lambda$, where R is the distance of the observation from the aperture and r is the radius of the aperture. The Fresnel approximations are commonly used in studying the diffraction

phenomena of light, and because of the short wavelength of light, they can easily be satisfied in most of the cases.

In principle, the intensity distribution arisen from diffraction effect can be calculated by the Rayleigh Sommerfeld integral. By taking either the Fresnel or Fraunhofer approximations, the calculations of the diffraction integral can be simplified. Obviously, the resulting theoretical predictions are correct only in certain region which is determined by the approximation. The valid regions for the Fresnel and Fraunhofer approximations are shown in Fig. 2-4 [Samir et al., 2003; Milster, 2009]. As no approximation is taken, the Rayleigh Sommerfeld integral remains valid in the entire space to the right of the aperture plane, which is called Rayleigh Sommerfeld region. The term far field usually refers to the Fraunhofer region while near field can be considered as the region between the aperture plane and the Fresnel region.

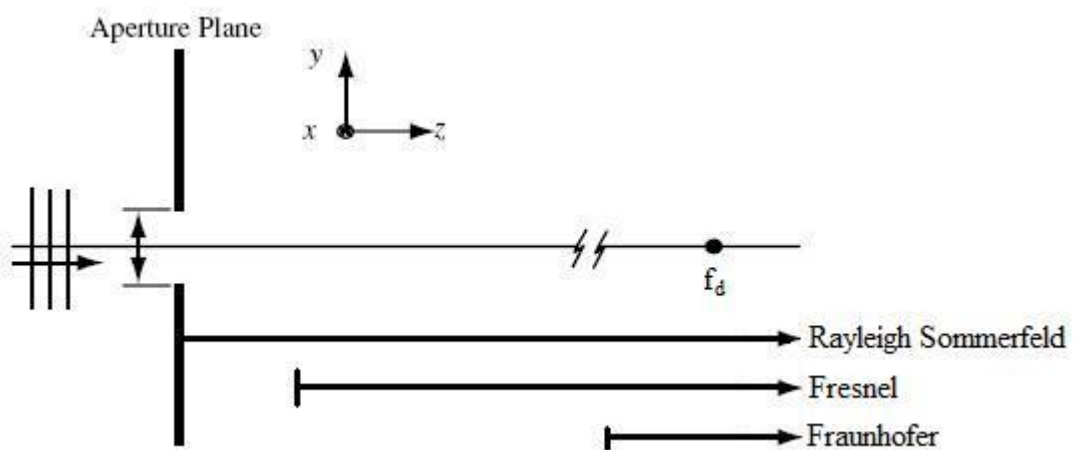


Fig. 2-4 The three diffraction regions: Rayleigh Sommerfeld region, Fresnel region and Fraunhofer region.

According to the Fresnel approximations, focal points other than the principle focal point (F_d) are found. At those "harmonic" (higher diffracted order) focal points, the path difference



between the waves from the center and the edge of the central circular electrode equals $(2j+1)(\lambda/2)$, where j is a non-zero integer. The relation between those focal lengths L_{2j+1} to L_d is given as [Zhang, 2005]:

$$F_{2j+1} = \frac{F_d}{2j+1} \quad (2-5)$$

The minimum distance of the observation point from the aperture Z_o is given by [Milster, 2004]:

$$Z_o = \sqrt[3]{\frac{\pi}{4} \lambda \left(\frac{r}{\lambda} \right)^4} \quad (2-6)$$

where λ is the wavelength in the medium, r is the radius of the aperture (i.e. the outer radius of the outmost annular electrode of the acoustic Fresnel zone plate).

In this work, it is planned to fabricate a self-focused piezoelectric transducer operating at ~ 4 MHz for ejecting drops of viscous liquids, e.g. glycerin (sound velocity = 1920 m/s). For practical considerations, the designed focal length L_d is about 10 mm and the outer radius of the outermost annular electrode (r) is about 6 mm. According to Eq. 2-6, the minimum distance from the transducer (i.e. aperture) is about 13 mm. This indicates that the working region (~ 10 mm from the transducer) is not in the Fresnel region. Because the difference is not very large, Eq. 2-3 is used in this work for calculating the dimensions of the annular electrodes.

2.2 Fabrication of the Fresnel zone plates

Lead zirconate titanate (PZT) ceramic plates (America Piezo 880) of thickness 0.5 mm were used as the piezoelectric actuating elements for fabricating the FZPs. The observed

thickness mode resonance frequency of the PZT plates was 4.28 MHz, which was the operating frequency of the focused acoustic ejectors. The inner and outer radii of the annular electrodes were calculated using an acoustic wavelength of 0.448 mm and a designed focal length of 10 mm by Eq. 2-3. Since it is aimed at ejecting drops of viscous liquid, glycerin was used as the liquid medium for investigation in this work. Hence, a wave velocity of 1920 m/s for glycerin was used to calculate the wavelength at the operating frequency (4.28 MHz). FZPs with 6, 5 and 4 annular electrodes (including the central electrode) were used for the study. Silver electrodes, in the pattern of the Fresnel zones, were applied on the PZT plates by screen printing.

Since only the piezoelectric material covered by the annular electrodes is excited by the external electric field, the resulting vibrations will be hindered by the un-excited material next to it, thus giving a smaller vibration amplitude. The effect will be more severe for the outer and thinner electrodes. In order to reduce the hindrance, non-electroded regions on the PZT plate were milled to a thickness of 0.35 mm. A photograph of the "milled" FZPs is shown in Fig. 2-5. Ordinary FZPs of uniform thickness of similar structures were also prepared for the comparison.



Fig. 2-5 Photograph of a milled FZP



Chapter 3 Characterization of the Fresnel Zone Plates

Before the fabrication of the focused acoustic ejectors, the self-focusing performances of the Fresnel zone plates (FZPs) are first evaluated. A needle-type hydrophone was used to measure the pressure (or intensity) distribution of the acoustic waves in glycerin generated by the FZPs. On the basis of the results, the positions with maximum intensity (i.e. focal points) were determined.

3.1 Measurements of intensity distribution

A hydrophone is an electro-acoustic sensing device for measuring the acoustic pressure at a particular position in a liquid medium. The hydrophone consists of a piezoelectric thin film as the sensing element for detecting the acoustic pressure associated with the incident acoustic wave. The piezoelectric thin film converts the acoustic pressure to an electrical voltage. The voltage generated by the hydrophone is linearly proportional to the pressure, so the pressure and hence intensity distribution of the acoustic wave can be determined, in terms of the observed voltage from the hydrophone.



In this work, the variation of the intensity is resulted from wave interference, and hence it is finer than the acoustic wavelength which is 0.448 mm (sound velocity = 1920 m/s, operating frequency = 4.28 MHz). In order to resolve such a fine distribution, a hydrophone with a sensing element smaller than the wavelength (e.g. 0.2 mm) should be used. If a hydrophone with a large sensing element is used, the fine distribution will be smoothed out and some details will be lost. However, it is very difficult to fabricate a hydrophone with a so small sensing element (0.2 mm), and the receiving sensitivity may also be not high enough for the accurate measurement. Making a compromise between the fabrication and resolution, a hydrophone with a sensing element of diameter 0.5 mm (with a housing of diameter 0.8 mm) was used in this work for the measurement. The sensing element of the hydrophone was a poled P(VDF-FrFE) copolymer film with a thickness of 6 μm [Chan, 1999]. Indeed, although the actual distribution of the intensity may not be obtained, it is expected that the self-focusing phenomena and the focal points can still be observed.



3.2 Experimental setup

The schematic diagram of the experimental setup is shown in Fig. 3-1. To evaluate the self-focusing performance, the Fresnel zone plate FZP was attached to the end of a cylindrical container as shown in Fig. 3-1. The container was filled with glycerin (with a viscosity of 1400 cP [Grigoriev et al., 1997]) to a depth of 30 mm (designed focal length L_d of the FZP is 10 mm). A signal generator (Sony Tektronix AFG 310) was used to generate a sinusoidal voltage at a frequency of 4.28 MHz and a voltage of 10 V, for driving the FZP. The voltage applied on the FZP V_a was measured by a digital oscilloscope (HP Infinium). The needle-type hydrophone was immersed in glycerin with its surface aligned parallel to the surface of the FZP. The hydrophone was able to translate in three orthogonal directions (along the axial direction and parallel to the surface of the FZP). The voltage generated by the hydrophone V_h was amplified by a matched preamplifier (National Physical Laboratory) and then measured by the digital oscilloscope. The ratio of V_h/V_a was used to study the intensity distribution of the acoustic wave.

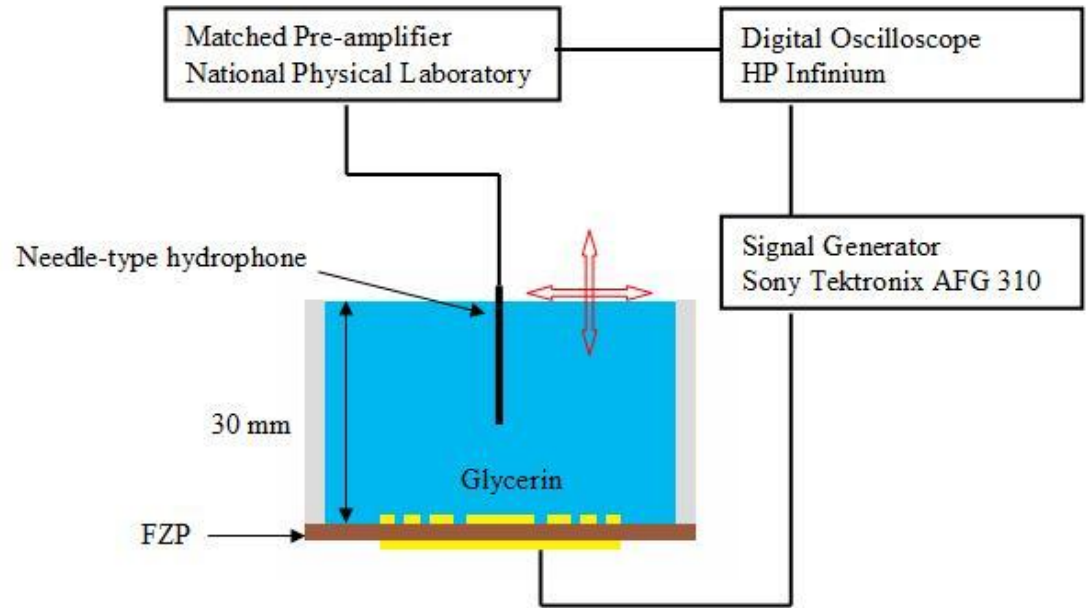


Fig. 3-1 Schematic diagram of the experimental setup to measure the intensity distribution of the acoustic waves in the glycerin

3.3 Results and discussion

3.3.1 Axial intensity distribution

Fig. 3-2 shows the variations of intensity (in terms of V_h/V_a) along the axial direction for the milled FZP with six annular electrodes (including the central circular electrode). Three focal points where the intensity becomes maximum were observed; they are labeled as F_a (2.48 mm from the plate), F_b (6.18 mm mm from the plate) and F_c (9.5 mm from the plate). It should be noted that the active element of the hydrophone was about



0.5 mm in diameter, which was larger than the wavelength of the acoustic wave, so the measurement only gave the averaged intensity at the position. As a result, the measurements did not show a sharp maximum at the three focal points.

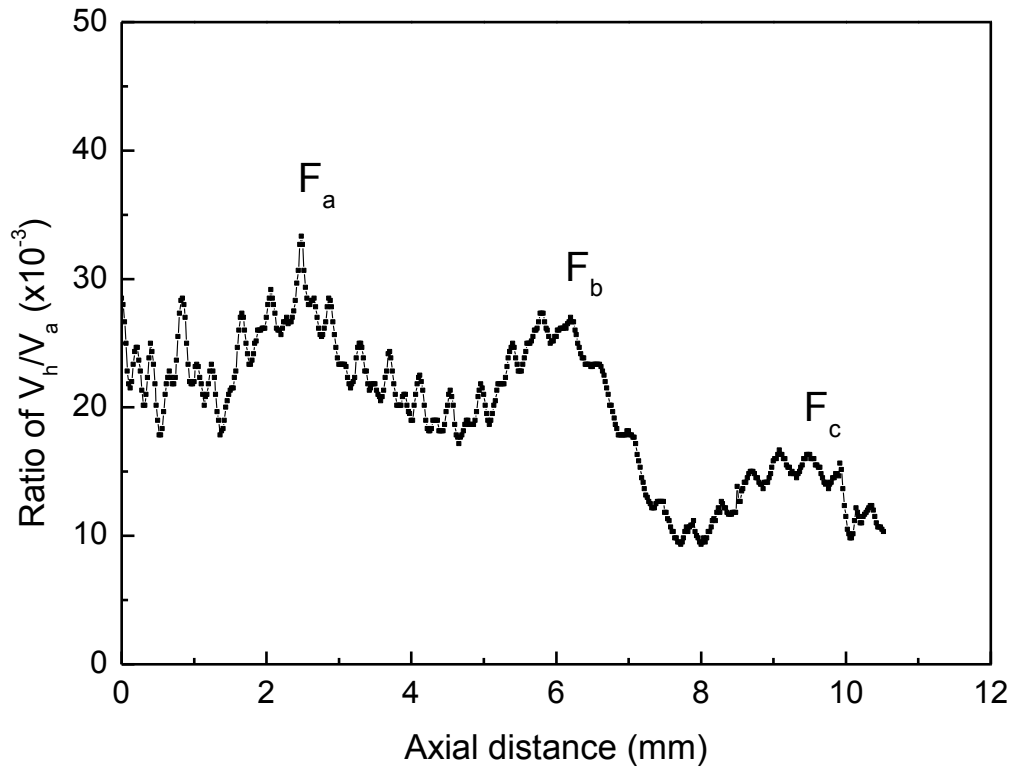


Fig. 3-2 The variations of intensity (in terms of V_h/V_a) along the axial direction for the milled FZP with six annular electrodes (including the central circular electrode)

Apparently, the observed focal points F_c should be the principle focal point, corresponding to the designed focal point F_d . There is only small difference between the designed focal length L_d (10 mm) and the observed focal length L_c (9.5 mm). The other



two focal points should be resulted from the constructive interference at higher orders.

The observed focal point F_a should be the third-order (principle) maxima, at which the path difference between the waves from the (adjacent) edges of the annular electrodes equals 1.5λ . The observed focal point F_b should be the secondary maxima located between the first-order (i.e. F_c) and third-order principle maxima.

It has been shown that the attenuation of an acoustic wave propagating in a liquid is dependent on its viscosity and density. The attenuation coefficient of glycerin (with a viscosity of 1400 cP) is about 200 times larger than that of water (1 cP) [Grigoriev, 1997; Kujawska, 2004]. A calculation has shown that the penetrations depth for a 4-MHz acoustic wave traveling in glycerin is about 8 mm [Rife, 2000; Ko, 2007]. That may be reason for the lower intensity at F_c as compared to that at F_a .

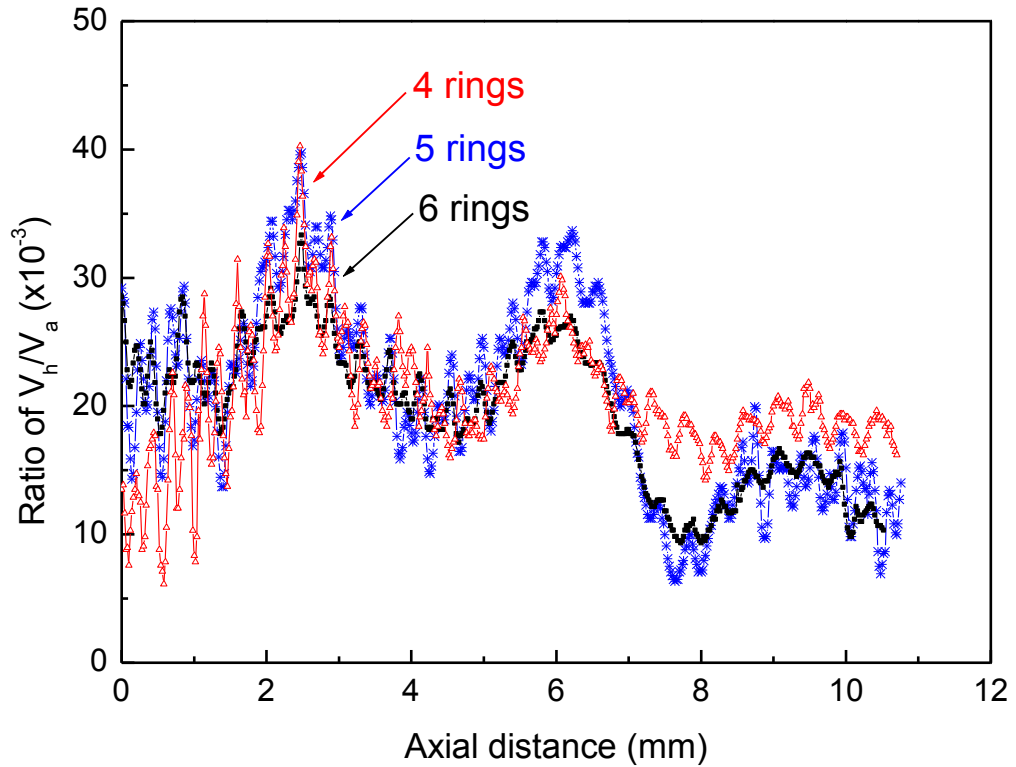


Fig. 3-3 The axial distributions of intensity for the FZPs with six (---■---), five (---*---), four (---△---)

annular electrode

The axial distributions of intensity of the FZPs with five and four annular electrodes are shown in Fig. 3-3, in which the distribution for the FZP with six annular electrodes is also plotted for comparison. Except for the distribution around the principle focal point, there is basically no difference between the distributions. As the number of the annular electrodes decreases, the principle focal point becomes unclear. This may be due to the decrease in the number of waves participating in the constructive interference. Due to the



high attenuation, the waves arriving at this region become relatively weak, having only a small amplitude.

Because of the high intensity, the higher order focal point F_a (at ~ 2.5 mm), instead of the principle focal point F_c (at ~ 10 mm) was chosen in this work for the ejection of viscous liquids. Accordingly, the FZP with four annular electrodes (including the central circular electrode) was selected for the fabrication of the focused acoustic ejector. In addition to the smaller dimension (~ 12 mm for the plate with four annular electrode versus ~ 16 mm for the plate with six annular electrodes), the FZP also gives a higher intensity under the same driving voltage (not V_a), probably due to the larger impedance and hence better matching with the signal generator.

3.3.2 Transverse intensity distribution

The variations of intensity (in terms of the V_h/V_a) at F_a and normal to the axial direction for the milled FZPs are shown in Fig. 3-4. Basically, there is no major difference between the distributions for the plates with six, five and four annular electrodes. Probably due to more waves be involved in the interference, the sidelobes (i.e. the shoulders around 0.5 - 3 mm) for the FZP with six annular electrodes become noticeable. It can be seen that the intensity for all the plates decreases drastically from the central of the plate, having a very



small value at distances larger than 1 mm from the axis. This clearly indicates that the acoustic wave is effectively focused and the corresponding focal point is very small, about 1 mm in diameter. As discussed before, the observed intensity is an averaged value over a small area of 0.5 mm, so the actual focal point should be smaller than 1 mm. In general, the dimension of the focal point is determined by and has the same order of magnitude of the wavelength which is 0.448 mm.

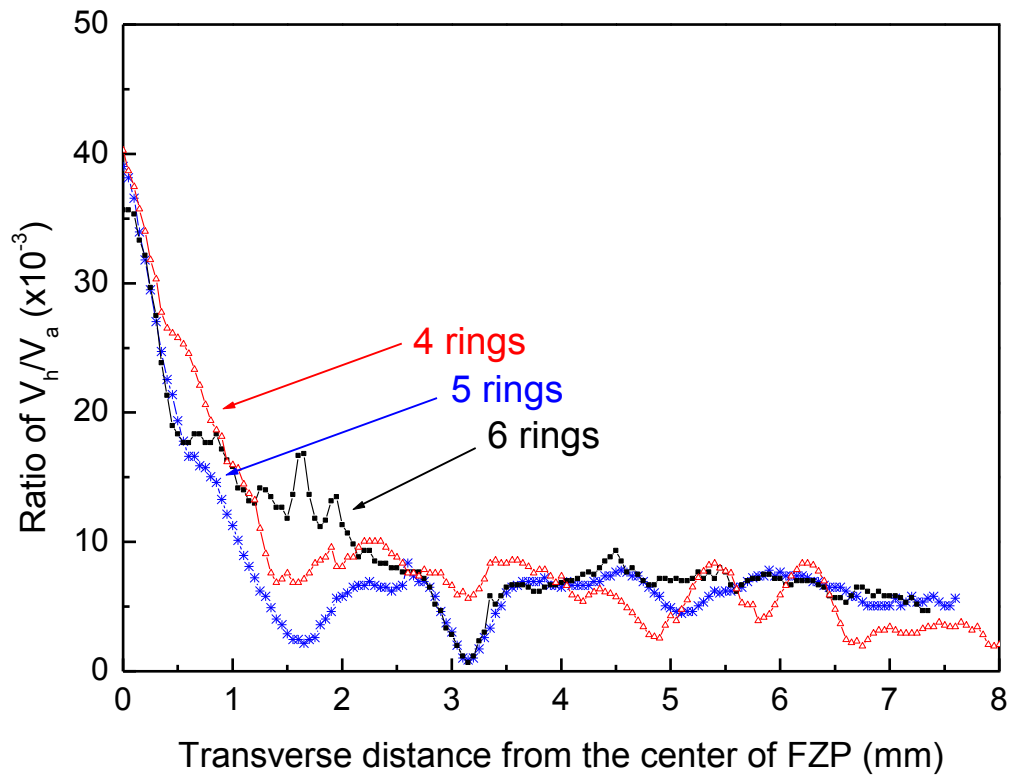


Fig. 3-4 The variations of intensity (in terms of V_h/V_a) along the lateral direction for the milled FZPs with six (---■---), five (---*---), four (---△---) annular electrodes



3.3.3 Comparison of the milled and non-milled FZPs

As discussed in Chapter 2, the vibrations generated by the piezoelectric materials covered by the annular electrodes will be hindered by the un-excited materials next to it, and the hindrance will be more severe for the outer and thinner electrodes. Hence milled FZPs were prepared. To study the effects arising from the hindrance, non-milled FZP with four annular electrodes was fabricated and characterized.

Fig. 3-6 (a) and Fig. 3-6 (b) show the axial and transverse intensity distributions (in terms of V_h/V_a) for the non-milled FZP. The distributions for the milled FZP are also plotted in the figures for comparison. As shown in Fig. 3-6 (a), two focal points, F_a and F_c , are observed for the non-milled FZP. The corresponding focal lengths are almost the same as those for the milled FZP. However, it is noted that no focal point F_b is observed for the non-milled FZP and the principle focal point is more noticeable.

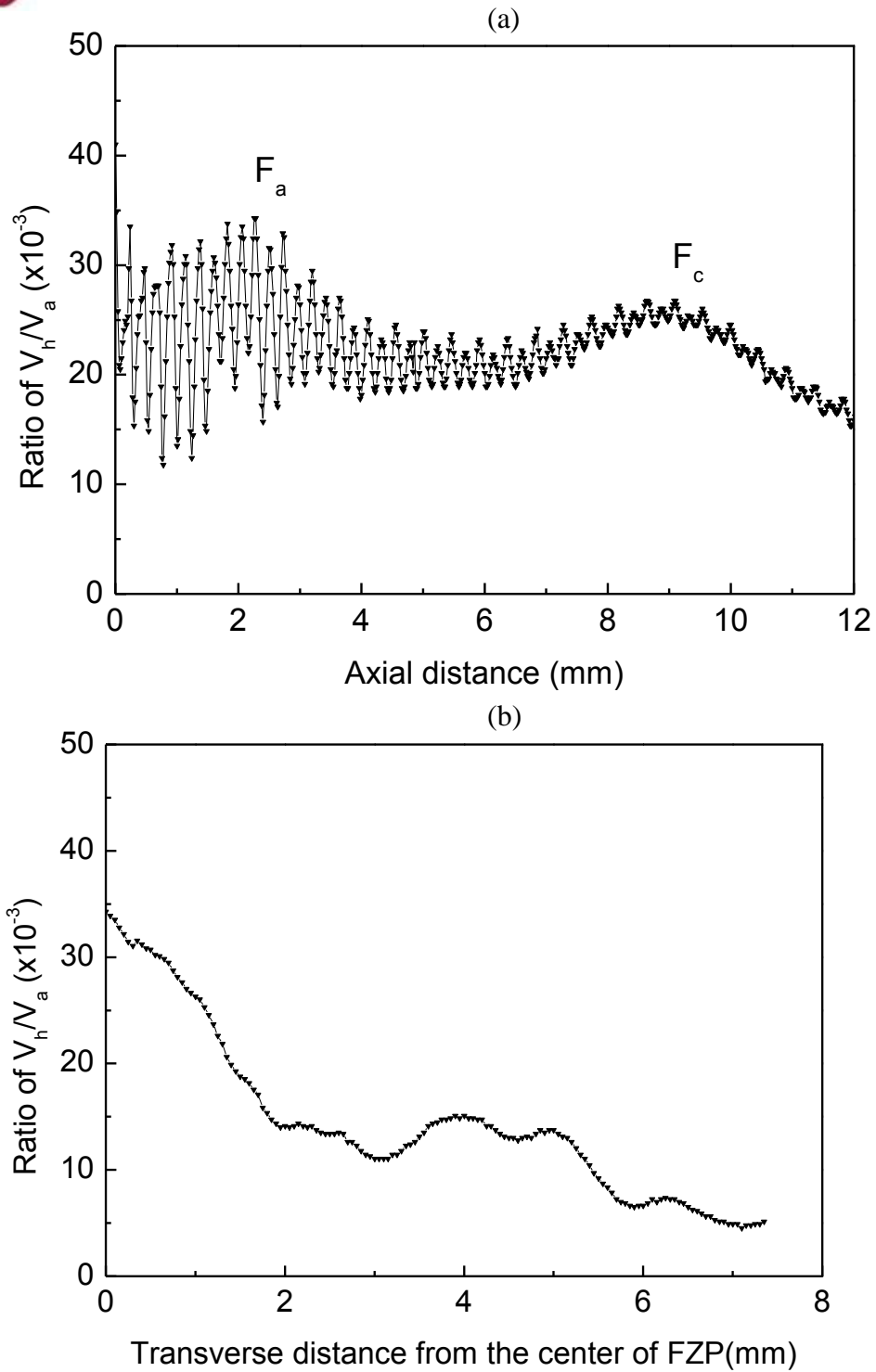


Fig. 3-5 The variations of intensity (in terms of V_h/V_a) along the (a) axial direction and (b) transverse direction for the non-milled FZP with four annular electrodes

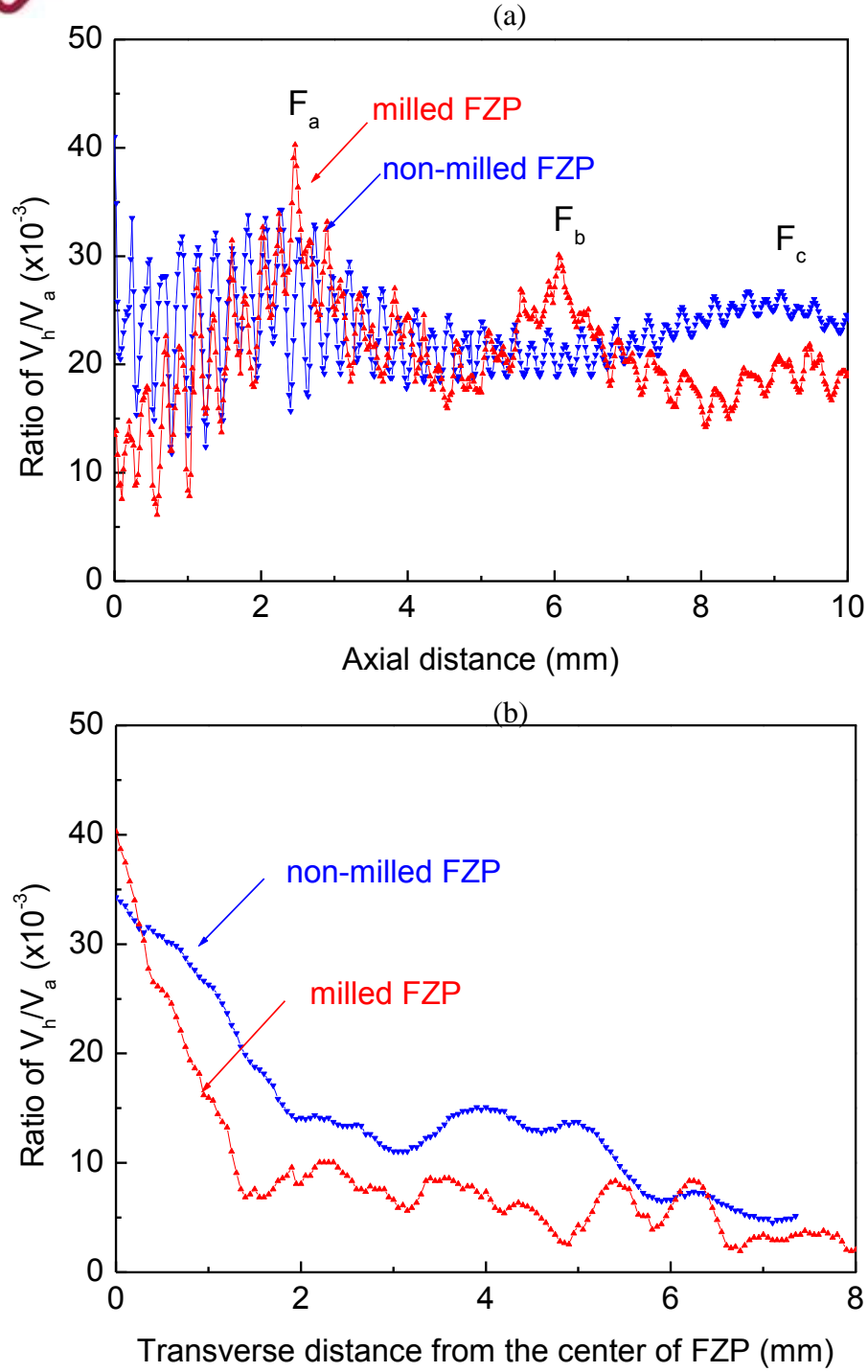


Fig. 3-6 Comparisons of the variations of intensity (in terms of V_h/V_a) along the (a) axial direction and (b)

transverse direction for the non-milled ($--\blacktriangledown--$) and milled ($--\blacktriangle--$) FZPs with four annular electrodes



It is also noted that the intensity of the non-milled FZP is close to that of the milled PZT. This seems to show that the hindrance by the un-excited material is not significant. However, it is suggested this should be due to the different electric fields applied to the FZPs. Although the voltage (V_a) used to excite both the milled and non-milled FZP is the same, the actual electric field across the plates may not be the same. For the milled FZP, the piezoelectric materials, which has a very high dielectric constant (1700), is surrounded by air. Due to the large difference in dielectric constants, the fringing of the electric field at the edge is significant, making the electric field inside the piezoelectric material become smaller. Unlike the milled FZP, the excited piezoelectric material in the non-milled FZP is surrounded by the same piezoelectric material. Hence, the fringing of the electric field is relatively small, and the electric field inside the material becomes larger than that in the milled FZP. Therefore, it is suggested that if both the non-milled and milled FZPs are driven by the same electric field, the vibration of the non-milled FZP is smaller. This makes the resulting intensity become lower and the variation of the intensity smaller. The 5th order diffraction of focal point of the central electrode becomes blurred. As a result, there is a relatively small difference between the intensities at F_a and F_c , and no F_b which is the integration of higher order focal point and increasing intensities.



It is also suggested that, due to the hindrance, the vibrations from the outer electrodes are also very small. As a result, the wave cannot be focused effectively, giving a large focal point and a larger sidelobe as shown in Fig. 3-6(b).

In conclusion, the Fresnel zone plate shows the self-focusing phenomena with focal points at 2.5 mm, 6.18 mm and 9.5 mm. Due to the attenuation of glycerin, the maximum intensity of the focused acoustic wave was found at 2.5 mm. Besides, the size of the FZP can be reduced, without deteriorating the focusing effect, by using lesser annular electrodes. Moreover, the milled FZT shows better focusing effect than the non-milled FZT. Therefore, milled FZT with four annular electrodes was used as a focused piezoelectric transducer for the fabrication of focused acoustic ejectors.



Chapter 4 Fabrication and Characterization of Focused Acoustic Ejectors

4.1 Fabrication of focused acoustic ejectors

In most of the previous works, ejection of liquid drops in an upward direction is demonstrated. However, this could not be directly applied in practical applications, which need to eject drops in a downward direction. In this work, it is therefore planned to design a focused acoustic ejectors for ejecting liquid drops in downward direction. The schematic diagram of the ejectors is shown in Fig. 4-1. As discussed in Chapter 3, because of the high intensity and small size, the milled FZPs with four annular electrodes were used as a focused piezoelectric transducer for the fabrication of focused acoustic ejectors. The FZP was mounted, with an air-backing, to a cylindrical metal holder. The assembly was then fastened to a cylindrical tube, in which it can be rotated to move upwards and downwards so as to adjust the vertical position and then the liquid depth. The other end of the cylindrical tube was sealed with a thin metal plate, at the center of which there is a small orifice of diameter 1.0 mm. A hole with a diameter of 4 mm was opened at the side of the cylindrical tube for filling (and refilling during the operation) the chamber with liquid.

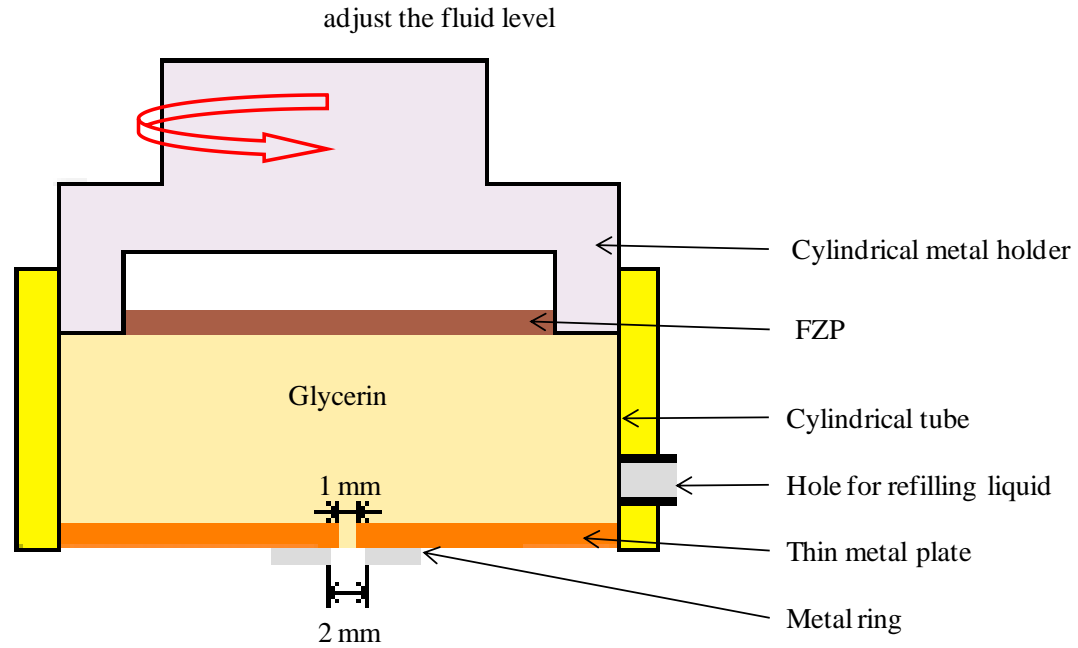


Fig. 4-1 Schematic diagram of the focused acoustic ejector in downward ejection

4.2 Characterization of focused acoustic ejectors

The schematic diagram for evaluating the ejection performances of the focused acoustic ejectors is shown in Fig. 4-2. A signal generator (Sony Tektronix AFG 320) was used to generate a wave train composing of a series of tone-bursts, each of which has a voltage V_o , an operation frequency f_{op} and a duration T (Fig. 4-3). The repetition frequency of the tone-bursts is f_{rep} . The wave train was amplified using a power amplifier (NF Electronic Instrument 4055) before applying to the FZP. A digital oscilloscope (Sony Tektronix TDX 220) was used to measure the voltage applied on the FZP. The ejection process was recorded using a high-speed digital camera (Casio FX 1). The camera can



take 1200 pictures in a second, which is fast enough to record the details of the ejection process at a repetition frequency of 120 Hz.

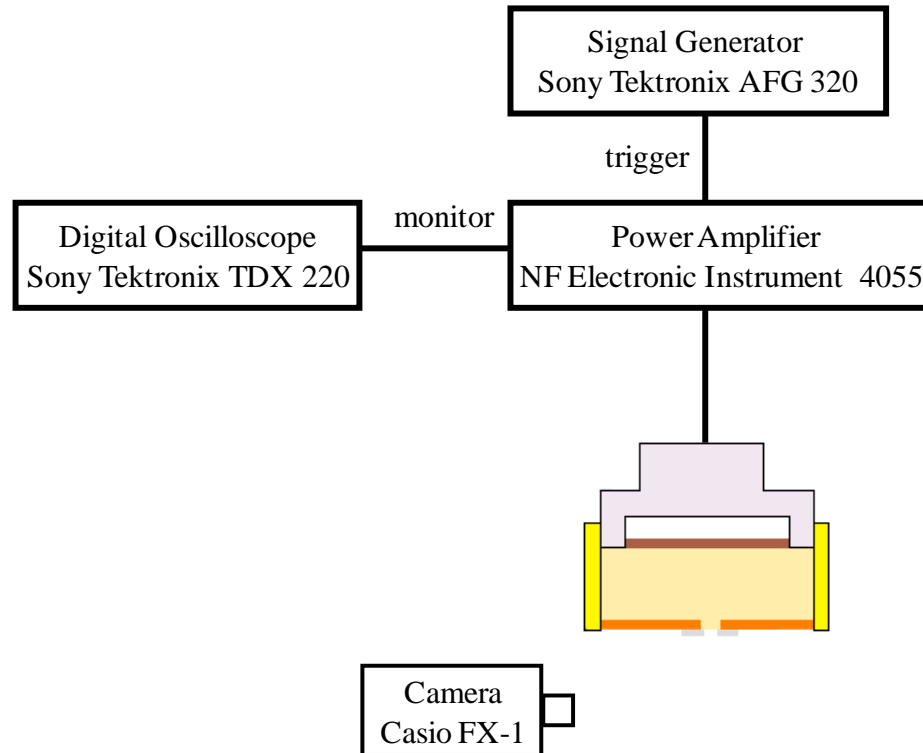


Fig. 4-2 Schematic diagram of the experimental setup for evaluating the ejection performances of the focused acoustic ejectors

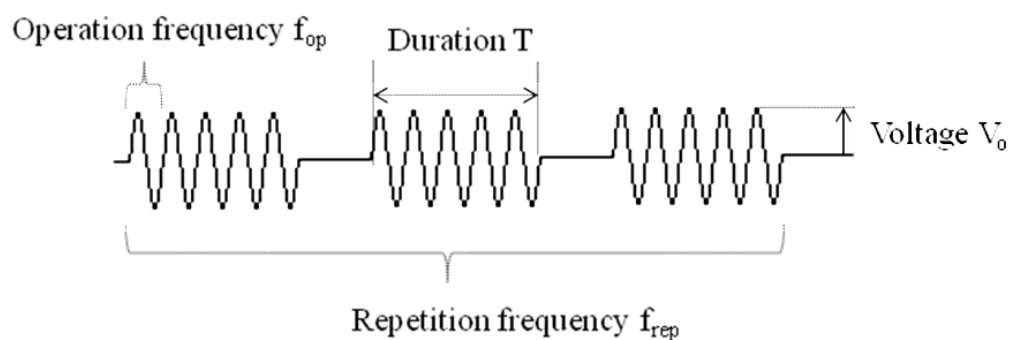


Fig. 4-3 The wave train comprising of a series of tone bursts with repetition frequency f_{rep} . Each tone burst



has voltage V_o , operation frequency f_{op} and duration T .

4.3 Results and discussion

4.3.1 Upward ejection

Before evaluating the capability of downward ejection, the ejector, without sealing of its thin metal plate, was first operated for upward ejection so as to study the self-focusing capability of the FZP and to locate the focal points. Tone-bursts with the same operation frequency of 4.28 MHz but different voltages (V_o) and durations (T) were applied to the ejector. In the upward orientation, the chamber of the ejector was filled with glycerin (with a viscosity of 1400 cP) to different depths, varied in steps of 0.125 mm.

It was observed that glycerin drops could be ejected only at the liquid depth of either 2.5 mm or 6.2 mm, which agrees with the observed focal points (F_a and F_b) in the intensity distribution measurements (Fig. 3-2). This indicates that the liquid-air interface did not have significant effect for the focusing of the acoustic waves. Fig. 4-4 shows photographs for the drop ejection at 2.5 mm and 6 mm.

The voltage V_o of the tone-burst used for the ejections at both F_a and F_b was 35 V.



However, the duration T used for the ejection at F_a was 2 ms, while that for the ejection at F_b was 3 ms. This indicates that a tone-burst of higher energy is required to eject drop at F_b . This agrees with the results of the intensity distribution measurement which shows that the wave intensity at F_b is lower than that at F_a . It is noted that although F_b is an “artificial” focal point, the enhanced intensity is high enough to eject drops of viscous glycerin from the surface.

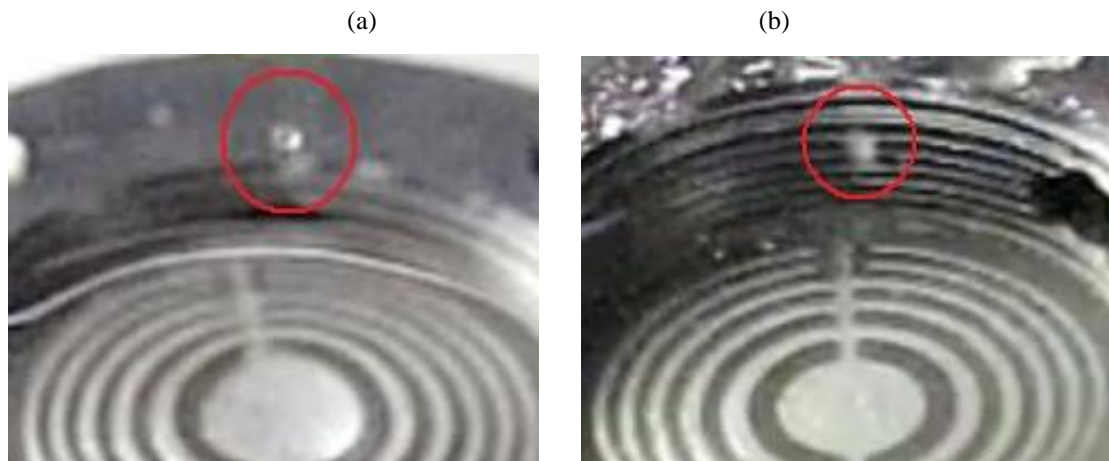


Fig. 4-4 Both positions of (a) 2.5 mm and (b) 6 mm allow drop ejection

Apparently, the liquid depth is the most important parameter for the focused acoustic ejector to have the drop ejection. It has been observed that if the liquid depth is not at the focal length, the liquid at the surface is deformed or displaced, forming a crest moving outwards as shown in Fig. 4-5. The height and the dimension of the crest are dependent



on the energy of the tone-burst (i.e. V_0 and T) and the liquid depth. However, if a tone-burst of higher energy is used, the crest will only become large, but a drop cannot be formed. It is probably because the cross-section of the deformed liquid is so large that it cannot break to form a drop. On the other hand, at the focal point, the intensity is large and the area of the deformed liquid (i.e. focal spot area) is small, such that it can be break easily to form a drop. Obviously, if the focal spot area is decreased, the size of the liquid drop will decrease.

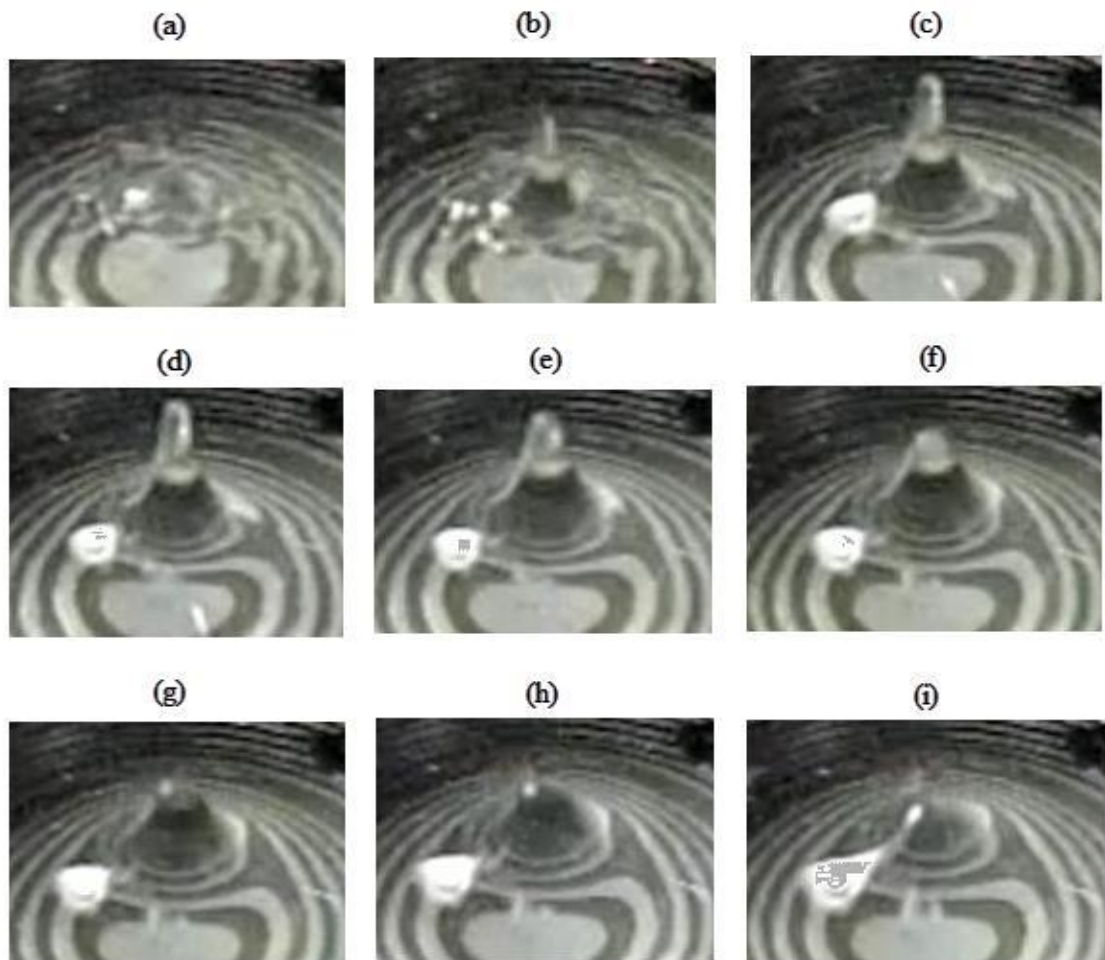




Fig. 4-5 When the liquid depth is not at the focal length (which is higher than L_b), the liquid at the surface is deformed without forming a drop, even though the higher energy of tone burst is used ($V_o = 40$ V and $T = 3$ ms). Photographs (a)-(i) shows the liquid surface deformation with time. Each photograph was taken with time step of $1/600$ s.

4.3.2 Downward ejection

After the evaluation of the ejection capability, the ejector was sealed with the thin metal plate and evaluated for the downward ejection. Because of the high intensity, the liquid depth of 2.5 mm (i.e. L_a) was selected for the ejection. Based on the results of the upward ejections, tone-bursts with an operation frequency f_{op} of 4.28 MHz, a voltage V_o of 35 V and a duration T of 2 ms were applied on the FZP. Using a liquid depth of 2.5 mm as a reference, the liquid depth was adjusted for the ejection. It was found that the liquid depth for downward ejections was the same as that for upward ejections. Similarly, this indicated that the thin metal plate did not have significant effect for the focusing of the acoustic waves. To evaluate the capability of the ejection in the drop-on-demand mode, a series of the tone-bursts (i.e. a wave train as shown in Fig. 4-3) were applied on the FZP. It was found that the ejector could eject glycerin drops one by one, following exactly the repetition of the tone-bursts (in drop-on-demand). The maximum repetition frequency was 120 Hz, which is fast enough for the practical applications. A photograph showing



the downward ejection of glycerin drops at such a high repetition frequency is shown in Fig. 4-6, while the operation parameters are summarized in Table 4-1. As shown in Fig. 4-6, there is a thin metal ring adhered at the outside of the orifice in the thin metal plate. The ring has a hole with an inner diameter of 2 mm larger than that of the orifice in the metal plate, and can help to eliminate the accumulation of liquid on the metal plate. The effects of the metal ring will be discussed in Section 4.3.3.4



Fig. 4-6 Downward ejection of glycerin drops in the drop-on-demand mode by the focused acoustic ejector. The operation parameters for the ejection are listed in Table 4-1

Table 4-1 Operation parameters for the focused acoustic ejector to eject glycerin drop in the drop-on-demand mode. The focused acoustic ejector is fabricated using the milled FZP with four annular electrodes.



Liquid viscosity (glycerin)	1400 cP
Liquid depth (i.e. focal length)	2.5 mm
Operation frequency (f_{op})	4.28 MHz
Voltage amplitude (V_o)	35 V
Duration (T)	2 ms
Maximum repetition frequency ($f_{rep,max}$)	120 Hz
Droplet diameter	0.4 mm

The observed diameter of the drops is about 0.4 mm, which is smaller than the wavelength of the acoustic wave (0.448 mm calculated using $f_{op} = 4.28$ MHz and sound velocity of glycerin = 1920 m/s). It has been shown that the focal spot area and then the droplet diameter are determined by the acoustic wavelength [Elrod et al., 1989; Huang et al., 2001; Lee et al, 2008]. Table 4-2 compares the normalized droplet diameter, which is defined as the ratio of the droplet diameter to the acoustic wavelength, in this work with those reported in the other works. It can be seen that most of the normalized droplet diameters are smaller than 1, and that in our work is almost the smallest one. These indicate that the acoustic waves are effectively focused to a small focal spot in our cases. It has been found that the droplet size was also affected by the energy of the tone-burst. A tone-burst with excess energy will cause the enlargement of droplet size that will be discussed in Section 4.3.3.1.



It should be noted that the amplitude of the electric field applied to the FZP for the ejection is 0.07 kV/mm, which is about 2% of the electric field used to polarize the piezoelectric plate. This suggests that a higher electric field can be applied to the FZP without causing any depolarization or damage to the piezoelectric material. Thus, by using a higher electric field, the focused acoustic ejector can generate more power for ejecting more viscous fluid, such as epoxy.

Table 4-2 Normalized droplet diameters for different works.

	Normalized diameter
Our work	0.83
Huang et al. (2001)	2.00
Yu et al. (2004)	0.79
Lee et al. (2006)	0.84
Lee et al. (2008)	1.07

Because of the high attenuation, the "harmonic" focal point was used instead of the principle focal point for the ejection. Therefore, if a shorter designed focal length is used, the intensity available for the ejection could be increased.



4.3.3 Effects of the operation parameters

4.3.3.1 Driving voltage

Driving voltage is the fundamental operation requirement for the drop ejection (Fig. 4-3).

Electrical energy that is fed into the piezoelectric material of the FZP converts to mechanical energy for the generation of acoustic wave in the liquid. Driving voltage is proportional to the acoustic wave energy. Sufficient acoustic wave energy can overcome the surface tension of liquid. In other words, there exists a threshold voltage for the drop ejection.

For the cases where the driving voltage is below the threshold value, vibration at the liquid surface is observed. In upward ejections, a small crest is formed at the liquid surface in response to the excitation of acoustic wave (Fig. 4-7(a)). Because of gravity, it disappears after the excitation. In downward orientation, the liquid at the orifice forms a meniscus. A meniscus with a good shape is required for the ejection (Fig. 4-7(b)), which will be discussed in the following section. During the ejection, the meniscus is elongated and then returns back.

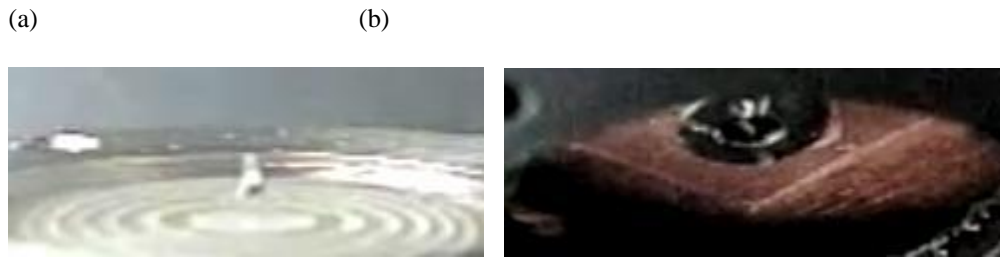


Fig. 4-7 Photographs showing the deformation of liquid under a driving voltage which is below the threshold value. (a) Upward ejection; and (b) Downward ejection.

In general, a high driving voltage will generate acoustic wave of higher intensity, and hence is preferred for the ejection. However, it has been observed that there exists a range of the driving voltage for ejecting drops in the drop-on-demand mode. Within the range, as the driving voltage increases, the droplet size increases. Moreover, the velocity of the ejected drop in downward ejections increases (Fig. 4-8). The velocity of the ejected drop was measured from the photographs taken by the high-speed camera. In upward ejections, the ejected drop reaches a higher position as the driving voltage increases (Fig. 4-9). When the voltage exceeds the range, satellite drops are formed as shown in Fig. 4-10(c). Sometimes, drops ejected at an angle from the vertical are also formed. If a very large voltage is applied, the ejection becomes a chaotic spray with a random direction. The drop ejection may also be stopped because of the undesirable accumulation of liquid at the orifice.



For the downward ejection of glycerin using a wave train with $T = 3$ ms, the range of V_o is from 36 V to 40 V.

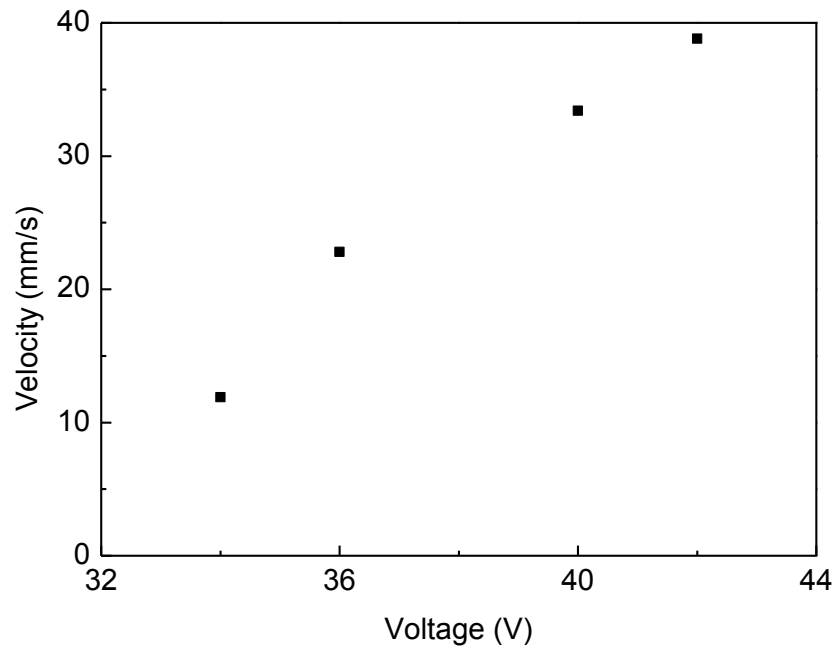


Fig. 4-8 Variation of the velocity of the ejected drops with the driving voltage.

(a)

(b)

(c)



Fig. 4-9 The maximum height that drop can reach at (a) 30 V (b) 35 V (c) 40 V with $T = 2$ ms

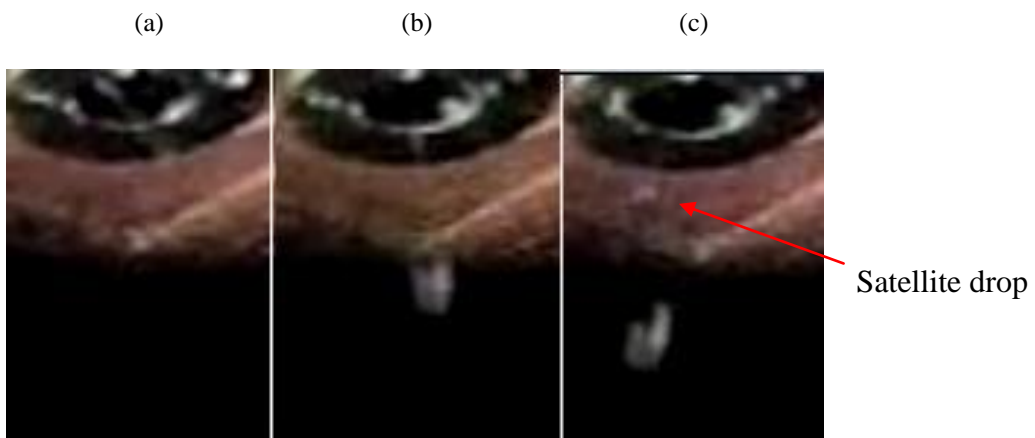


Fig. 4-10 Glycerin ejection with driven voltage of (a) 34 V (no drop ejection), (b) 36 V (formation of monodisperse drop) and (c) 43 V (drop accompanying with satellite drop)



4.3.3.2 Tone-burst duration

The tone-burst duration is the length of time that a sinusoidal wave of voltage from a signal generator is applied to the ejector (Fig. 4-3). Each tone-burst corresponds to the ejection of a single drop. The duration does not change the intensity of the focused acoustic wave at the liquid surface, but provides an enough destabilized time for the deformed liquid to form a discrete drop. It has been observed that, with a fixed driving voltage, a long duration can help to realize the drop ejection.

In general, the increase of the tone-burst duration increases the droplet size but does not affect the velocity of the ejected drop (for downward ejections) as shown in Fig. 4-11. A long duration makes more liquid become destabilized such that a larger drop is formed. As the acoustic energy per unit of the deformed liquid is the same, the velocity of drops in downward ejections remains almost unchanged. However, as the deformed liquid becomes larger, more satellite drops may be formed. If the tone-burst duration is too long, the deformed liquid forms a column, instead of a drop, as shown in Fig. 4-12. The column can be as high as 10 - 20 mm. The column is formed to balance the instability for reaching an equilibrium stage. However, as the acoustic energy per unit of the deformed



liquid does not increase, the surface tension cannot be overcome to eject a drop.

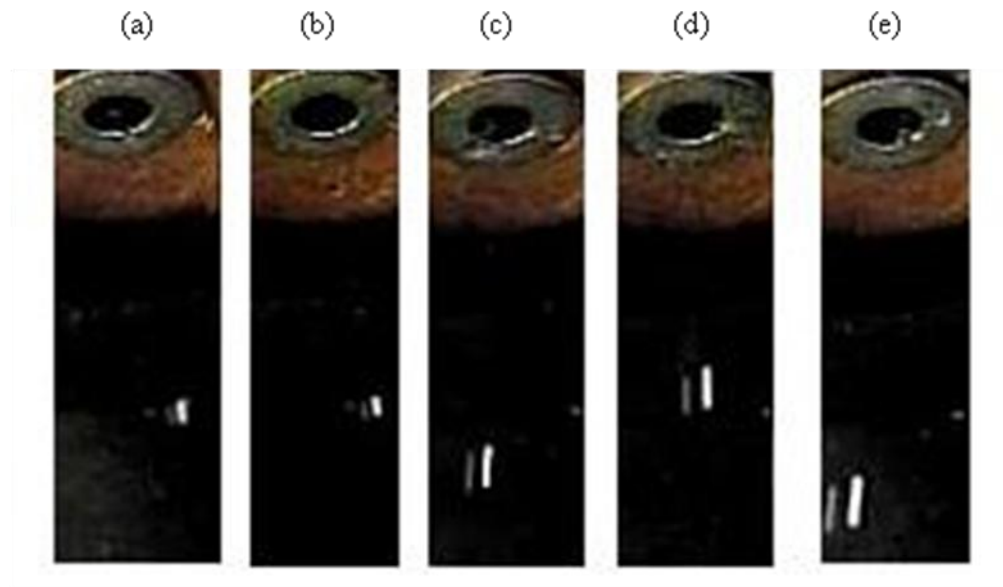


Fig. 4-11 Change of droplet size with tone-burst duration of (a) 1ms (b) 2ms (c) 3ms (d) 4 ms (e) 5ms in

downward ejection at the same driving voltage.





Fig. 4-12 The deformed liquid forms a column with height of 10-15 mm with $T = 5$ ms and $V_o = 40$ V

Apparently, if the tone-burst duration increases continuously, the wave train (Fig. 4-3) become a continuous sinusoidal wave. If a continuous sinusoidal wave with a high voltage is applied to the FZP, liquid drops cannot be ejected in the drop-on-demand mode. Moreover, the FZP will be overheated, resulting in a dramatically shift of the resonance frequency and then the stop of the drop ejection. Therefore, tone-bursts with finite duration as well as appropriate separation (i.e. repetition frequency) are required for the drop ejection in the drop-on-demand mode.

4.3.3.3 Repetition frequency

For the drop-on-demand mode operation, it is expected that a liquid drop can be ejected by each tone burst. Repetition frequency of the tone-burst then determines the ejection rate of the drops (Fig. 4-3).

In general, there is no minimum limitation of the repetition frequency for our focused acoustic ejectors. As our ejectors do not utilize nozzles for the ejection, there does not



exist the so-call "the first drop problem" which is common for the liquid ejectors utilizing a nozzle [Lee, 2002]. For those liquid ejectors, the print head (containing the nozzle) will be blocked by liquid that has solidified after sitting there for a long period of time. The drop ejection is then not allowed unless pulses with higher energy are applied. In our ejectors, the orifice is mainly used to prevent leakage of the liquid. It does not affect the size of the ejected liquid drops. Therefore, a very small orifice (such as the nozzle) is not required, and hence there does not exist the so-called "the first drop problem". By using the optimized conditions, our ejectors can function at any time.

On the other hand, the maximum repetition frequency is limited by the duration of the tone burst. As discussed in the previous section, it cannot be too high that the wave train becomes a continuous wave or the FZP is overheated. It is also limited by the formation the desired meniscus. A meniscus with a good shape is required for a stable drop ejection, which will be discussed in the following section.

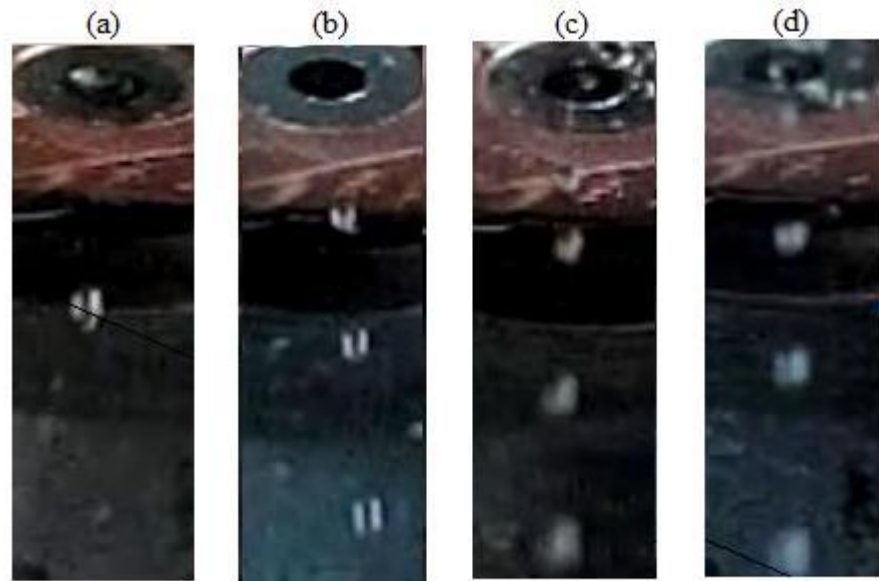


Fig. 4-13 Downward ejection of different repetition frequency of (a) 50 Hz (b) 80 Hz (c) 100 Hz (d) 120 Hz with the same $V_o = 35$ V and $T = 2$ ms.

The maximum repetition frequency is also limited by the velocity of the ejected drops. The initial velocity of the drop is controlled by the voltage. As the drop travels in air, it is decelerated rapidly. Therefore, if the repetition frequency is too high, the drops will collide with each other and then individual drop cannot be obtained. In other words, the ejection is no longer in the drop-on-demand mode.

In this work, the driving voltage was first maximized for the drop ejection and the duration of the tone-burst was then minimized. At last, the repetition frequency was



maximized for the ejection in the drop-on-demand mode.

4.3.3.4 Pressure

The external pressure applied to the liquid through the side-hole of the cylinder tube (Fig. 4-1) plays an important role in the ejection process. The pressure constitutes the atmospheric pressure and the pressure due to the weight of the liquid in the reservoir. It determines the shape of the liquid at the orifice, i.e. the meniscus, which is a crucial factor for the drop ejection. For instance, an excessive pressure makes a considerable amount of liquid accumulate at the rim of orifice, which will usually stop the drop ejection because of the increase in the liquid mass. If drops do get ejection, they are large and satellite drops are also formed. However, if the pressure is not large enough, the liquid seems to be pull back and hence liquid drops cannot be ejected.

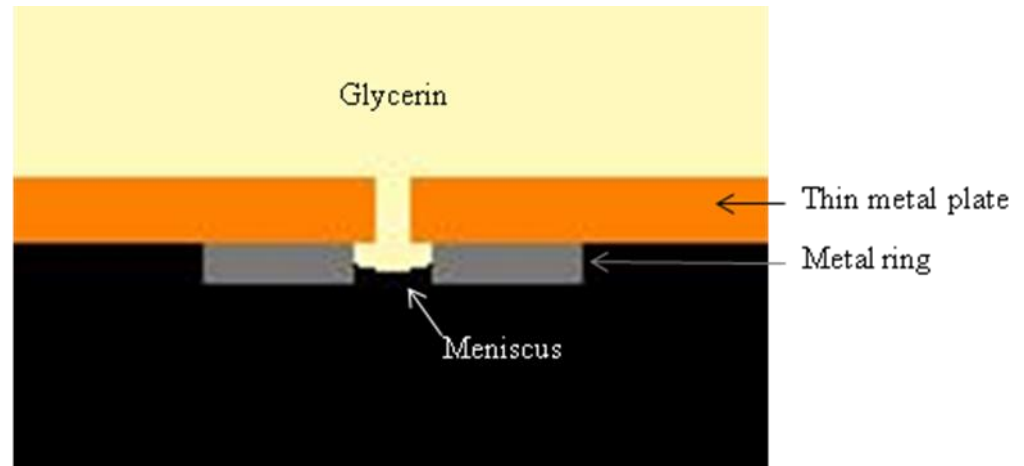


Fig. 4-14 Schematic diagram of the desired shape of the meniscus at the orifice needed for the drop ejection

It has been observed that a good shape of the meniscus (Fig. 4-14) is required for the drop ejection. A thin metal ring (with inner diameter of 2 mm) fixed concentrically at the outside of the orifice can help to build up such a shape of the meniscus. The liquid tends to bind by the ring instead of affixing to the surface of the metal plate arbitrarily. If the liquid affixes to the metal plate, the amount as well as the shape of the liquid are arbitrary and cannot be controlled as shown in Fig. 4-15 (a). As a result, the size and the moving direction of the ejected drops are quite random. Ejected drops moving nearly parallel to the plate have been observed. With the ring, the shape and amount of the liquid at the orifice can be adjusted by changing the pressure (through changing the liquid in the reservoir or the height of the reservoir).

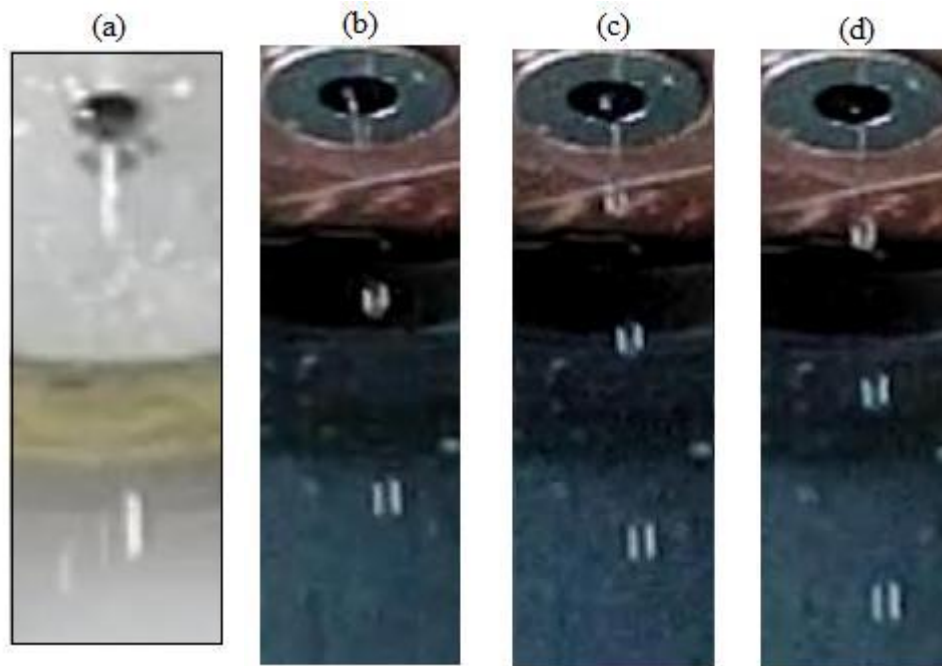


Fig. 4-15 Meniscus shape of downward ejection of the ejector (a) without metal ring (b) with metal.

Photographs (b)-(d) showing the change of shape of meniscus with time during ejection (with time step of 1/600 s)

A constant pressure is required to refill the liquid during the ejection process; and obviously, a high pressure is required for the ejection at higher repetition frequency. In this work, the pressure was kept constant by fixing the position of the reservoir and the amount of liquid inside. Obviously, it is better to have a control system, instead of a manual approach, to maintain the constant pressure, and this improvement may be



incorporated in the future work.

4.3.4 Effects of the ejector design

4.3.4.1 Orifice size

In this work, orifices of different diameter and different shapes have been used for the ejection. It has been observed that the droplet size is not affected significantly by the diameter and shape of the orifice in the thin copper cover plate. On the other hand, the orifice cannot be too small to disturb the deformation of the liquid by the focused acoustic wave. The orifice should be slightly larger than the area of the focal spot; and its major function is to prevent the leakage of the liquid.

4.3.4.2 Operation frequency

The thickness mode resonance frequency of the piezoelectric plate of the FZP is chosen as the operation frequency of the ejector. At the resonance frequency, the amplitude of vibration in the thickness direction is the largest, and hence generating acoustic waves with the highest amplitude. The operation frequency determines the wavelength of the



acoustic wave, which controls the focal spot area at the liquid surface and then the size of the ejected liquid drops [Elrod et al., 1989; Lee et al., 2008]. It has been shown in Section 4.3.2 that the diameter of the glycerin drops ejected by the ejector operated at 4.28 MHz is about 0.4 mm, which is about 0.8 times of the acoustic wavelength (0.448 mm). To investigate the relation between the acoustic wavelength and the droplet size, focused acoustic ejector operated at 2.14 MHz has been fabricated following similar procedures. Our results show that the diameter of the ejected drops is about 1 mm (Fig. Fig. 4-16), which is very close to the wavelength of the acoustic wave in glycerin (0.90 mm). This agrees with the theoretical work that the minimum droplet size is about the wavelength of the acoustic wave. The result indicates that the acoustic wave (in the ejector operated at 2.14 MHz) is also focused effectively. On the basis of the results (including those for orifice size), it can be concluded that the droplet size is mainly wavelength and then the operation frequency of the ejector.



Fig. 4-16 Downward ejections at different operation frequencies of (a) 2.14 MHz (b) 4.28 MHz.

4.3.4.3 Milling of the Fresnel zone plates

As discussed in Chapter 3, the vibration of the piezoelectric material covered by the annular electrodes is hindered by the un-excited material next to it. As a result, the intensity of the acoustic wave generated by the non-milled FZP is weaker than that by the milled FZP. Moreover, as the vibration of the outer electrodes is very small due to the heavier hindrance, the acoustic wave cannot be focused effectively. As a result, the focal point becomes larger than that of the milled FZP, and the sidelobe become larger. The non-milled FZP with four annular electrodes has been used to fabricate the focused acoustic ejector, and its performance in ejection has been measured and compared with that of the ejected fabricated using a milled FZP.



As shown in Fig. 4-17, ripples are formed in the glycerin surface near the central focal spot for the ejector with the non-milled FZP. This should be attributed to the large sidelobes observed in the transverse intensity measurements (Fig. 3-6). Although the intensity of the acoustic wave generated by the non-milled FZP is weaker than that by the milled FZP, it is interesting to note that the operation conditions for both ejectors using the non-milled and milled FZP are the same. i.e. $V_o = 35$ V and $T = 2$ ms. This should be partly due to the averaged measurements of the intensity by the hydrophone which has a large sensing element (0.5 mm in diameter). This may also indicate that the cover and then the reflection at the cover may help the ejection.



Fig. 4-17 Photographs were taken from the ejector with (a) non-milled FZP and (b) milled FZP. Ripples were observed in glycerin surface near the central focal spot for the ejector with non-milled FZP



4.3.4.4 Thin copper cover plate

As shown in Fig. 4-1, a thin copper plate with an orifice at the center is used to seal the cylindrical tube to form a chamber for the liquid. The other function of the copper plate is to cool the liquid, preventing it from reaching a high temperature. Because of the focusing, the wave intensity at the focal points increases significantly (Fig. 3-3). Especially at high repetition frequencies, e.g. 90 Hz, the liquid may get heated, which is not desirable for epoxy or other heat-sensitive liquids. For epoxy, heating can initiate the cross-linking between the macromolecules, making the epoxy in the chamber become partially cured. This will affect the normal curing process which will be carried out subsequently, or even make the epoxy in the chamber become completely cured and hence clog up the chamber if the operation time is too long. It has been observed that at a high repetition frequency of 90 Hz and a driving voltage of 35 V, the temperature at the focal point (measured on the glycerin through the orifice) is about 50°C. Moving away from the focal point in a transverse direction, the temperature (measured on the copper plate) decreases gradually and becomes constant at about 30°C at distance larger than 2 mm. However, if a poor condition such as plastic cover plate (PMMA) is used, the temperature at the focal point is about 75°C. The temperature (measured on the plastic



plate) around the focal point decreases only slowly with the distance from the focal point and still has at a relatively high value of 40°C at the edge of the ejector.

It has also been observed that, for the copper cover plate, if the repetition frequency is decreased to 70 Hz, the temperature at the focal point decreases slightly to about 48°C, and the temperature around the focal point remains at about 30°C. Unlike the copper cover plate, the temperature at the focal point remains high at 65°C if a plastic cover plate is used, and the temperatures around the focal point still exceed at above 40°C. This indicates that the temperature of the liquid is strongly dependent on the repetition frequency, and the copper can effectively cool the liquid to below 50°C, irrespective of the repetition frequency.

4.3.4.5 Number of Fresnel zones

As discussed in Chapter 3, the wave intensities (in terms of V_h/V_a) for the milled FZP with four, five and six Fresnel zones or annular electrodes are the same. However, it has been noted that, probably due to the different impedances and then different loadings to the signal generator, the voltage applied to the FZP (measured by the digital



oscilloscope) is smaller than the setting of the signal generator; and the difference becomes larger if the number of the Fresnel zones increases. In other words, if a constant voltage (setting of the signal generator) is applied, the actual wave intensity for the FZP with four annular electrodes is the largest (about 60% larger than that for the FZP with six annular electrodes).

The ejectors using the milled FZP with four, five and six annular electrodes have been fabricated and evaluated for the ejection performances. Table 4-3 summarizes the operation conditions for the ejectors. All the three ejectors can eject glycerin drops in the drop-on-demand mode, with the droplet size about 0.4 mm. In consistent with the above discussion, the driving voltage V_o used for the ejector using the FZP with four annular electrodes is the smallest, while the duration T is the shortest. It should be noted that the driving voltage V_o of the wave train is the setting of the signal generator. As also shown in Chapter 3, the focusing capabilities for the three FZP are similar, all producing a fine focal spot. Because of the largest wave intensity and good self-focusing capability, the FZP with four annular electrodes has then been selected in this work for the fabrication of the ejector. Moreover, the resulting ejector is more compact in size.



Table 4-3 Operation condition for ejectors with different number of annular electrodes

Number of annular electrodes	4	5	6
Driving voltage (V)	70	70	90
Tone burst duration (ms)	2	3	3

4.3.4.6 Air bubbles

The design of the ejector as well as the operation must be good enough to make sure that there is no air bubbles trapped in the liquid. Air bubbles in the liquid have adverse effects on the drop ejection. Acoustic impedance of air is much smaller than that of the liquid, such as glycerin. Acoustic wave propagating toward the air bubbles will be mostly reflected at the interfaces. As a result, the focusing of the wave becomes worse. If air bubbles are trapped at only one corner, the asymmetric focusing will cause the ejected drop to travel in a non-vertical direction. If air bubbles are trapped in most area or near the orifice, a larger driving voltage is required or the drop ejections will be stopped.



Air bubbles can be ingested into and trapped in the liquid in a number of different ways:

1. Air bubbles may be introduced into the fluid during the filling and refilling processes.

Care must be taken to ensure the all the air bubbles in the chamber, tubing and the reservoir are removed in the filling process. During the refilling process, care must be taken to ensure the reservoir is always full of the liquid.

2. Air bubbles may be ingested in the liquid through the orifice during the ejection process if the refilling rate is not fast enough. After a drop is ejected, a thin meniscus is remained at the orifice and has a tendency to move backward to the chamber. If the refilling process is not fast enough to make the meniscus form the desired shape, air bubbles will be formed at the orifice.

A transparent cylindrical tube or a transparent cover plate will be helpful in observing the air bubbles. Plastics, e.g. PMMA, should be a suitable choice for this requirement because of the low cost and the ease in machining. However, plastic is not good for heat conduction and then cooling of the liquid. As discussed in Section 4.3.4.4, a plastic cover plate will cause the liquid temperature to increase by about 20°C. It has been observed that a metal cover plate with a small hole sealed with a transparent plate is a practical method to provide both observation and cooling.



4.3.5 Ejection of various liquids

As discussed in Chapter 2, the dimensions of the annular electrodes of the FZP are dependent on the wavelength of the acoustic wave. Therefore, different FZPs should be used for ejecting drops of different liquids. However, it is of interest to know if other liquids can be ejected by the focused acoustic wave, so the ejector fabricated using the FZP which is designed for glycerin has been used, for trials, to eject other liquids, such as water, pre-polymer of epoxy and detergent. Apparent, the resulting operation conditions, as summarized in Table 4-4, are not the optimal. Also, for the ease of the trials, only the upward ejection has been evaluated for most of the liquids.

Table 4-4 Operation conditions for ejector ejecting various liquids

	Glycerin	Water	Pre-polymer of epoxy	Detergent
Driven voltage (V)	35	25	40	45
Pulse duration (ms)	2	1	2	8



Water

As compared to glycerin, a tone burst with lower energy, a driving voltage V_o of 25 V and a duration of 1 ms, is required to eject water drops using the ejector. As discussed in Chapter 1, in order to eject a liquid drop, the liquid is first stretched significantly until the surface tension is overcome. Therefore, both the surface tension and viscosity are important parameters governing the drop ejection. However, as the liquid has to be stretched significantly before forming a drop, the viscosity is more crucial than the surface tension in controlling the ejection. It is hence a tone-burst of higher energy is required to eject glycerin. Glycerin has a lower surface tension than water (63 vs 72 dyn/cm [Grigoriev et al., 1997]), and its viscosity is more than one thousand times larger than that of water (1400 versus 0.83 cP at room temperature [Grigoriev et al., 1997]).

Pre-polymer

A pre-polymer of epoxy (EE-7132A, Rapid Chemical, Taiwan) with a viscosity of ~2000 cP has been used for the trial of ejection. The epoxy is designed for LED encapsulation molding and fiber optical applications. As compared to glycerin and



water, it has a lower surface tension (~ 47 dyn/cm [May, 1988]) but a higher viscosity. As shown in Table 4-4, a tone-burst of larger energy ($V_o = 40$ V and $T = 2$ ms) is hence required for the ejection. Fig. 4-18 shows the upward ejection of pre-polymer of epoxy with time. As epoxy is commonly used in industries, the pre-polymer has also been evaluated for downward ejection. It has been observed that it can be effectively ejected in downward orientation and in the drop-on-mode demand mode (Fig. 4-19). The observed maximum repetition frequency is 80 Hz. It should be noted that the FZP is not designed for the pre-polymer, the operation conditions determined from the trials are hence not the optimal.

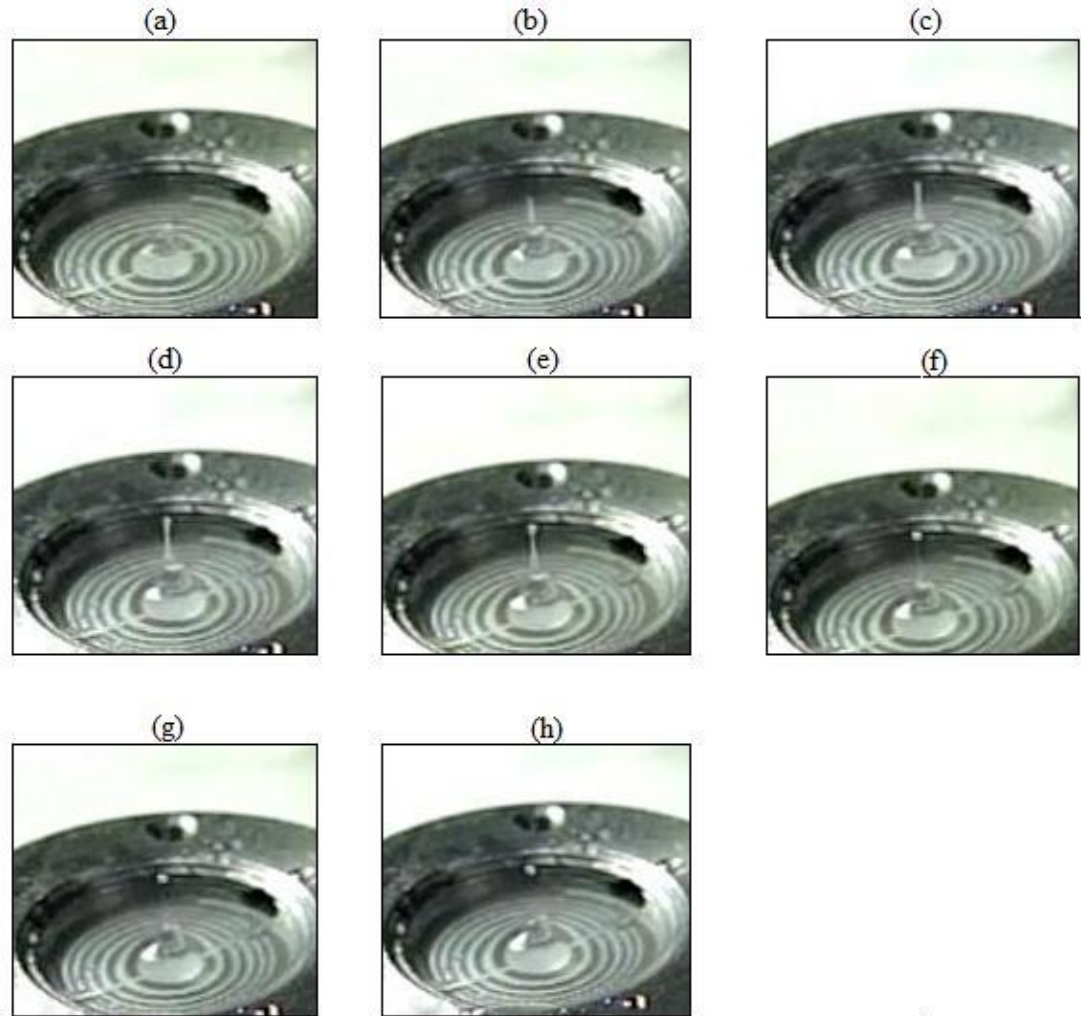


Fig. 4-18 (a)-(h) Upward ejection of pre-polymer of epoxy with time (Each photograph was taken with time step of 1/600 s). Operation conditions were shown in Table 4-4.

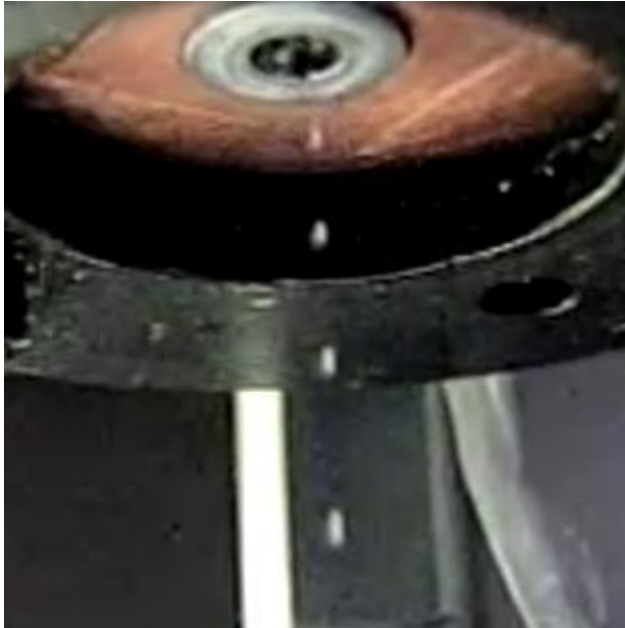


Fig. 4-19 Downward ejection of pre-polymer in drop on demand mode with $V_o = 40$ V, $T = 2$ ms and $f_{\text{req,max}} = 80$ Hz

On the basis of the results, it is suggested that viscosity is a more crucial parameter in controlling the drop ejection. For the ejection using the focused acoustic wave, the volume of liquid to be stretched is small and the intensity is enhanced (both determined by the focal spot). As a result, drops of liquids with a high viscosity can be formed and ejected. Our results also agree with the recent theoretical work which suggests that the pulse energy for drop ejection is proportional to the viscosity and inversely proportional to the surface tension of the liquid [Eggers, 1997].



Detergent

Detergent is a liquid generally having a low surface tension and high viscosity. The molecular structure of detergent is characterized by a polar group connected to a typically long hydrocarbon chain. Its polar groups make the intermolecular force between air-detergent interfaces become small [Broze, 1999]. Because of its long tail, the viscosity which is related to the molecular weight of the liquid is usually high. In this work, a detergent with a viscosity higher than that of glycerin has been used. As the viscosity of liquid cannot be measured in our laboratories, the viscosity of the detergent is estimated by experience.

As shown in Table 4-4, the energy of the tone burst for ejecting detergent is the highest. In particular, the duration of the tone burst is very long, about 8 ms. This should be attributed to the high viscosity and the low surface tension of the detergent. As shown in Fig. 4-20, the detergent can be stretched significantly by the focused acoustic wave. However, it seems that the energy is not large enough to overcome the friction between the molecules easily and hence break the liquid to form a drop. As a result, a high liquid column is formed. Probably with the assistance of the restoring force of the liquid, a

large drop is eventually formed.

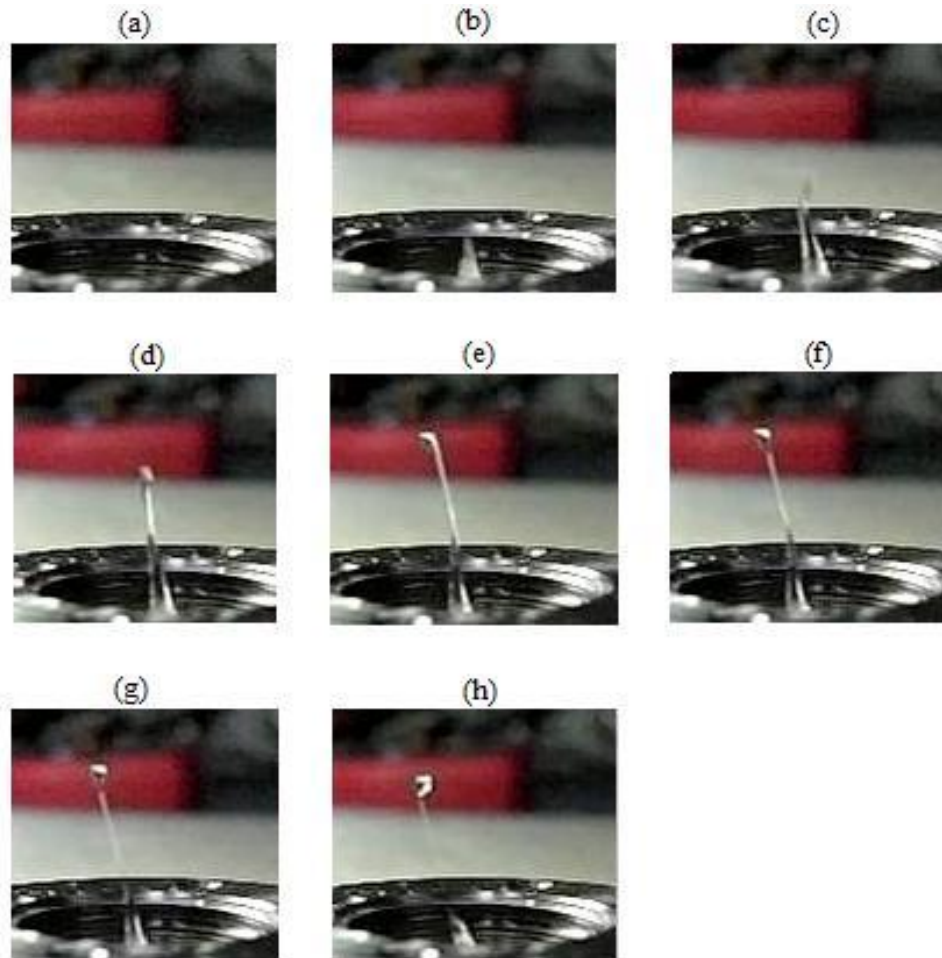


Fig. 4-20 (a)-(h) Upward ejection of detergent with time (Each photograph was taken with time step of 1/600 s). Operation conditions were shown in Table 4-4.

Although the observed ejection performances of other liquids are not the optimal, our results clearly indicate that the focused acoustic ejector is able to eject viscous liquids effectively. Since only a small volume of the liquid is stretched, the liquid can be



deformed effectively by the acoustic wave of which the intensity is greatly enhanced. As a result, drops of liquids with a high viscosity can be formed and ejected. Our results also suggest that viscosity is more important than surface tension in controlling the drop ejection.



Chapter 5 Conclusion

Focused acoustic ejectors using the Fresnel zone plates as the self-focusing piezoelectric transducers have been successfully developed and fabricated. Because of the enhanced intensity of the acoustic wave, the ejectors can effectively eject viscous liquids, such as glycerin (1400 cP) and the pre-polymer of an epoxy (2000 cP), in the drop-on-demand mode at a high repetition frequency of 120 Hz. The driving signals of the ejectors is simple, just a series of tone bursts of sinusoidal wave, and the size of the ejector is small, about 15 mm in diameter.

Milled Fresnel zone plates with different numbers of the annular electrodes have been designed and fabricated using lead zirconate titanate piezoelectric plates. The self-focusing capability of the Fresnel zone plates has been evaluated by the measurements of the wave intensity distribution using a needle-type hydrophone. The Fresnel zone plates are operated at 4.28 MHz, the thickness mode resonance frequency of the piezoelectric plate. Our results reveal that after the milling of the un-electroded region of the piezoelectric plate, the vibration and hence the wave intensity is enhanced. The acoustic wave is focused effectively by the constructive interference, giving a small focal spot with a diameter close to the wavelength of the acoustic wave (0.448 mm). The



observed focal lengths are about 2.48 and 9.5 mm, which agree with the theoretical values.

The number of the annular electrodes does not have not significant effects on the wave intensities. Our results also reveal that the attenuation of the acoustic wave in the viscous liquids is high, making the intensity at the principle focal point (9.5 mm) being smaller than that at the “harmonic” focal point (2.48 mm). On the basis of the results, the milled Fresnel zone plate with four annular electrodes is used as the self-focusing piezoelectric transducer for the ejectors, and the "harmonic" focal point is selected for the ejection operation.

The ejection performances of the focused acoustic ejectors using glycerin as the medium have been evaluated in detail. The effects of the operation parameters, including the driving voltage and duration of the tone burst, have been investigated. Based on the results, the optimum operation parameters have been determined. Our results reveal that the ejector can eject glycerin in the downward orientation using a tone burst with a frequency of 4.28 MHz, a driving voltage of 35 V and a duration of 2 ms. The drop is small, having a diameter of 0.4 mm which is close to the wavelength of the acoustic wave. Using the same operation parameters, the ejector can eject drops in the drop-on-demand mode. The repetition frequency can be increased to 120 Hz, while the temperature



remains at about 50°C.



References

- Amemiya, I., Y. Nomura, K. Mori, I. Takasu and S. Uchikoga, "LED Packaging by Ink-jet Microdeposition of High-Viscosity Resin and Phosphor Dispersion", SID 07 DIGEST, pp. 1603-1606 (2007)
- Bicerano, J., "Prediction of Polymer properties: second edition, revised and expanded", Marcel Dekker, Inc., New York, pp. 193-212 (2002)
- Broze, G., "Handbook of Detergent: Part A Properties," Marcel Dekker, Inc., New York, pp. 133-156 (1999)
- Chan, H. L. W., S. T. Lau, K. W. Kwok, Q. Q. Zhang, Q. F. Zhou and C. L. Choy, "Nanocomposite ultrasonic hydrophones", Sensors and Actuators A: Physical, Volume 75, Issue 3, pp. 252-256 (1999)
- Chen, J. Y. and W. M. Fan, "Measurement of Liquid Surface Tension Coefficient by using Si-Resistnace-Strain Gauge", Laboratory Research and Exploration, Vol. 21, No. 6 (2002)
- Demirci, U., "Acoustic Picoliter Droplets for Emerging Applications in Semiconductor Industry and Biotechnology", Journal of microelectronical system, vol. 15, no. 4 (2006)
- Demirci, U., "Acoutic Picoliter Droplets for Emerging Applications in Semiconductor Industry and Biotechnology", Journal of Microelectromechanical systems, Vol. 15. No. 4, pp. 957- 965 (2006)
- Demirci, U., G. Y. Geoksen, E. Haggstrom and B. T. Khuri-Yakub, "Femtoliter to Picoliter Droplet Generation for Organic Polymer Deposition Ejector Arrays", IEEE Transactions on Semiconductor Manufacturing, Vol. 18, No. 4, pp. 709-714 (2005)
- Eggers, J., "Nonlinear dynamics and breakup of free-surface flows", Rev. Mod. Phys. 69, pp. 865 (1997)
- Ellson, R., M. Mitchell, B. Browning, L. Lee, M. F. Miller and R. Papen, "Transfer of



Low Nanoliter Volumes between Microplates Using Focused Acoustics-Automation Considerations", JALA, pp. 29-34 (2003)

Elrod, S. A., B. Hadimioglu, B. T. Khuri-Yakub, E. G. Rawson, E. Richley and C. F. Quate, "Nozzleless Droplet Formation with Focused Acoustic Beams", Journal of Applied Physics, 65 (9), pp. 3441-3447 (1989)

Elrod, S. A., "Acoustic Lens Arrays for Ink Printing", U. S. Patent 4751530 (1986)

Ersoy, O. K., "Diffraction, Fourier Optics and Imaging", Wiley-Interscience, A John Wiley & Sons, Inc., pp. 25-82 (2007)

Forbush, M., "Effect of Focal Distance on Drop Volume in Acoustic Drop Ejection", EDC Biosystems leaflet, <http://www.edcbiosystems.com/>

Grigoriev, I. S. and E. Z. Milikhov, "Handbook of Physical Quantities", CRC press, pp.409-412, 451-459 (1997)

Hadimioglu, B., S. A. Elrod, D. L. Steinmetz, M. Lim, J. C. Zesch, B. T. Khuri-Yakub, E. G. Rawson and C. F. Quate, "Acoustic Ink Printing", Ultrasonic Symposium 1992, IEEE, pp. 929-935 (1992)

Hadimioglu, B., S. A. Elrod and R. Sprague, "Acoustic Ink Printing: An Application of Ultrasonics for Photographic Quality Printing at High Speed", Ultrasonic Symposium 2001, IEEE, pp. 627-635 (2001)

Harvey, J. E. and A. Krywonos, "Axial Irradiance Distribution throughout the Whole Space behind an Annular Aperture", Applied Optics, Vol. 41, No. 19, pp. 3790-3795 (2002)

Harvey, J. E. and A. Krywonos, "Axial Irradiance Distribution Throughout the Whole Space Behind an Annular Aperture: reply to comments", Applied Optics, Vol. 42, No. 19, pp. 3792-3794 (2003)

Hayes, D. J., W. R. Cox, and M. E. Grove, "Microjet printing of polymers and solder for electronics manufacturing", Journal of Electronics Manufacturing, 8, pp. 209-216



- Howkins, S. D., "Inkjet Method and Apparatus", U. S. Patent 4459601 (1982)
- Hristov, H. D., "Fresnel Zones in Wireless Links, Zone Plate Lenses and Antennas", Artech House, Boston, London, pp. 139-226 (2000)
- Huang, D. and E. S. Kim, "Micromachined Acoustic-Wave Liquid Ejector", Journal of Microelectromechanical Systems, Vol. 10, No. 3, pp. 442-449 (2001)
- Kanda, H., "Ultrasonic Transducer using Ultra High Frequency", U. S. Patent 4321696 (1980)
- Kawanami, S., M. Kurokawa, M. Taniguchi and Y. Tada, "Development of Phased-Array Ultrasonic Testing Pro", Technical Review, Vol.38, No.3, pp.121-125 (2001)
- Kino, G. S., "Acoustic Waves: Devices, Imaging & Analog Signal Processing", Prentice-Hall, Inc., Englewood, New Jersey, pp. 154-317 (2001)
- Ko, S. H., S. G. Ryu, N. Misra, H. Pan and C. P. Grigoropoulos, " Laser induced short plane acoustic wave focsuing in water", Applied Physics Letters 91,051128, pp.1-3 (2007)
- Kujawska, T. and J. Wojcik, "Dependence of non-linear ultrasound beam propagation on boundary conditions", Ultragarsas, Nr.4(53), ISSN 1392-2114 (2004)
- Kwon, J. W., H. Y. Yu, Q. Zou and E. S. Kim, "Directional Droplet Ejection by Nozzleless Acoustic Ejectors Built on ZnO and PZT", Journal of Micromechanics and Microengineering, 16, pp. 2697-2704 (2006)
- Kwon, J. W., Q. Zou, and E. S. Kim, "Directional Ejection of Liquid Droplets through Sectoring Half-Wave-Band Sources of Self-Focusing Acoustic Transducer", MEMS 2002, pp. 121-124 (2002)
- Lam, K. H., H. L. W. Chan, H. S. Luo, Q. R. Yin and Z. W. Yin, "Piezoelectrically



Actuated Ejector using PMN-PT Single Crystal", *Sensors and Actuators A*, 121, pp. 197-202 (2005)

Lee, C. Y., W. Pang, H. Y. Yu and E. S. Kim, "Subpicoliter Droplet Generation based on a Nozzle-Free Acoustic Transducer", *Applied Physics Letters* 93, 034104 (2008)

Lee, C. Y., H. Y. Yu and E. S. Kim, "Acoustic Ejector with Novel Lens Employing Air-Reflectors", *MEMS 2006*, Istanbul, Turkey pp. 170-173 (2006)

Lee, C. Y., H. Y. Yu, and E. S. Kim, "Nanoliter Droplet Coalescence in Air by Directional Acoustic Ejection", *Applied Physics Letters* 89, 223902 (2006)

Lee, E. R., "Microdrop Generation", CRC press, pp. 1-82 (2002)

Lewis, A., M. Reighard, and F. Suriawidjaja, "Non-contact Dispensing Achieves Practical Results", *SMT*, pp.66-67 (1999)

Li, J. D., G. L. Deng, "Technology Development and Basic Theory Study of Fluid Dispensing -a review", *Proceeding of HDP'04*, pp. 198-205 (2004)

Lovelady, K. T. and L. F. Toye, "Liquid Drop Emitter", U. S. Patent 4308547 (1979)

May, C. A., "Epoxy Resins: Chemistry and Technology, Second Edition", Marcel Dekker Inc., pp. 606-608 (1988)

Milster, T. D., "Basic Diffraction", College of Optical Sciences, University of Arizona (2009)

Mitchell, W. M., S. H. Lee and G. McLendon, "Droplet Dispensation from a Reservoir with Reduction in Uncontrolled Electrostatic Charge", U. S. Patent 0244778 (2007)

Percin, G., "Photoresist Deposition Without Spinning", *IEEE Transactions on Semiconductor Manufacturing*, Vol. 16, No. 3, pp. 452-469 (2003)

Pickett, S., P. Chaurand, R. Huang, R. Stearns, B. Browning, S. Hinkson, R. Ellson and R. M. Caprioli, "Acoustic Droplet Ejection Enables Precise Timing and Positioning for



Deposition of Matrix to Optimize MALDI Tissue Imaging", Poster #146, IMSC 2006, Prague, Czech Republic (2006)

Piracci, A. F., "Practical Production Applications for Jetting Technology", APEX, Long Beach, CA (2000)

Reis, N., C. Ainsley and B. Derby, "Viscoisty and Acoustic Behavior of Ceramic Suspensions Optimized for Phase-Change Ink-Jet Printing", J. Am. Ceram. Soc., 88 [4] 802-808 (2005)

Rife, J. C., M. I. Bell, M. N. Kabler, R. C. Y. Auyeung and W. J. Kim, "Miniature valveless ultrasonic pumps and mixers", Sensors and Actuators 86, pp. 135-140 (2000)

Samir M. and A. R. Harvey, "Validity of Fresnel and Fraunhofer Approximations in Scalar Diffraction", Journal Optics A: Pure Applied Optics, 5, pp. S86-S91(2003)

Schindel, D. W., A. G. Bashford and D. A. Hutchins, "Focusing of Ultrasonic Waves in Air using a Micromachined Fresnel Zone Plate", 1997 Ultrasonics 35 (4), pp. 275-285 6 (1997)

Sleva, M. Z., and W. D. Hunt, "Design and Construction of a PVDF Fresnel Lens", Ultrasonic Symposium 1990, IEEE, pp. 821-826 (1990)

Stemme, N. G. E., "Sheet", U. S. patent 3747120 (1972)

Sweet, R. G. , "Fluid Droplet Recorder", U. S. Patent 3596275 (1963)

Umezu, S., H. Suzuki, and H. Kawamoto, "Droplet Formation and Dropping Position Control in Electrostatic Inkjet Phenomena", Proc. IS&T's NIP21, pp. 283-285 (2005)

Wang, D. A., C. H. Cheng, Y. H. Hsieh and Z. X. Zhang, "Analysis of an Annular PZT Actuator for a Droplet Ejector", Sensors and Actuators A 137, pp. 330-337 (2007)

Wang, H., D. Xing and L. Z. Xiang, "Photoacoustic Imaging using an Ultrasonic Fresnel Zone Plate Transducer", Journal Physics D: Applied Physics 41, 095111, pp. 1-7 (2008)



Yu, H. Y., J. W. Kwon and E. S. Kim, "Chembio Extraction on a Chip by Nanoliter Droplet Ejection", *Lab Chip*, 5, pp. 344-349 (2005)

Yu, H. Y., J. W. Kwon and E. S. Kim, "Microfluidic Mixer and Transporter Based on PZT Self-Focusing Acoustic Transducers", *Journal of Microelectromechanical Systems*, Vol. 15, No. 4, pp. 1015-1024 (2006)

Yu, H. Y., Q. Zou and J. W. Kwon, "Liquid Needle", *Journal of Microelectromechanical Systems*, Vol. 16, No. 2, pp. 445-453 (2007)

Zhang, Y. and C. Zheng, "Axial Intensity Distribution behind a Fresnel zone plate", *Optics & Laser Technology*, Vol. 37, Issue 1, pp. Pages 77-80 (2005)

Zoltan, S. I. and S. Heights, "Pulsed Droplet Ejecting System", U. S. Patent 3683212 (1970)